Water mass-specificity of bacterial communities in the North Atlantic revealed by massively parallel sequencing

Hélène Agogué, Dominique Lamy, Phillip R Neal, Mitchell S Sogin, Gerhard J Herndl

Water mass-specificity of bacterial communities in the North Atlantic revealed by massively parallel sequencing.

Hélène Agogué[1¤ ϴ], Dominique Lamy[1,2 ϴ], Phillip R. Neal[3], Mitchell L. Sogin[3], Gerhard J. Herndl[1,2*]

[1] Dept. of Biological Oceanography, Royal Netherlands Institute for Sea Research (NIOZ), P.O. Box 59, 1790AB Den Burg The Netherlands

[2] Dept. of Marine Biology, University of Vienna Althanstraße, 14 A-1090 Vienna, Austria

[3] Josephine Bay Paul Center for Comparative Molecular Biology and Evolution, Marine Biological Laboratory, 7 MBL Street, Woods Hole, Massachusetts 02543, United States of America

[¤]Current address : Institut du Littoral et de l'Environnement, UMR LIENSs 6250, CNRS-Université de la Rochelle, 2 rue Olympes de Gouges, 17000 LA ROCHELLE France

ϴ **These authors contributed equally to this work.**

Keywords: bacterial diversity; massively parallel tag sequencing; North Atlantic Ocean; deep water masses, bacterial biogeography

[*] To whom correspondence should be addressed:
Gerhard J. Herndl
Dept. of Marine Biology
University of Vienna
Althanstraße, 14

,A-1090, Vienna, Austria
E-mail: gerhard.herndl@univie.ac.at
Fax number: +43(0)1 4277 9571

Running title: Bacterial assemblages in North Atlantic Ocean

Abbreviations: LDW, lower Deep Water; NEADW, Northeast Atlantic Deep Water; SACW, South Atlantic Central Water; LSW, Labrador Sea Water; NIW, Northern Intermediate Water; tCW, transitional Central Water; AAIW, Antarctic Intermediate Water; DOC, dissolved organic carbon; DON, dissolved organic nitrogen; AOU, apparent oxygen utilization; HNA, high nucleic acid; MDS, non-metric multidimensional scaling; CCA, canonical correspondence analysis.

ABSTRACT

Bacterial assemblages from subsurface (100 m depth), meso- (200-1000 m depth) and bathypelagic (below 1000 m depth) zones at 10 stations along a North Atlantic Ocean transect from 60°N to 5°S were characterized using massively parallel pyrotag sequencing of the V6 region of the 16S rRNA gene (V6 pyrotags). In a dataset of more than 830,000 pyrotags we identified 10,780 OTUs of which 52% were singletons. The singletons accounted for less than 2% of the OTU abundance, while the 100 and 1,000 most abundant OTUs represented 80% and 96%, respectively, of all recovered OTUs. Non-metric Multi-Dimensional Scaling and Canonical Correspondence Analysis of all the OTUs excluding the singletons revealed a clear clustering of the bacterial communities according to the water masses. More than 80% of the 1,000 most abundant OTUs corresponded to *Proteobacteria* of which 55% were *Alphaproteobacteria*, mostly composed of the SAR11 cluster. *Gammaproteobacteria* increased with depth and included a relatively large number of OTUs belonging to *Alteromonadales* and *Oceanospirillales*. The bathypelagic zone showed higher taxonomic evenness than the overlying waters, albeit bacterial diversity was remarkably variable. Both abundant and low-abundance OTUs were responsible for the distinct bacterial communities characterizing the major deep-water masses. Taken together, our results reveal that deep-water masses act as bio-oceanographic islands for bacterioplankton leading to water mass-specific bacterial communities in the deep waters of the Atlantic.

INTRODUCTION

Prokaryotes represent an important component of the marine plankton, comprising up to 70% and 75% of the total biomass in surface (Fuhrman *et al.* 1989) and deep (Aristegui *et al.* 2009) waters, respectively. They serve a fundamental role in mediating a wide range of biogeochemical cycles (Azam *et al.* 1983; Karl 2002). The introduction of molecular tools has substantially increased our knowledge about marine microbial community structure and has shown that the vast majority of environmental microbes represents novel taxa that have yet to be cultivated (Handelsman 2004; Olsen *et al.* 1986). High-throughput sequencing methods and pyrosequencing allow for efficient deep molecular sampling efforts of the microbial populations (Gilbert *et al.* 2009; Huber *et al.* 2007; Huse *et al.* 2008; Sogin *et al.* 2006) and sidestep the need to clone individual DNA molecules (Margulies *et al.* 2005). Furthermore, data from these massively parallel sequencing approaches provide an exhaustive description of the taxonomic affiliation of microbial community. This information forms the basis for estimating both the richness and evenness of the microbial populations present in the environment which are, in turn, essential to refine our knowledge on the biogeography of marine microbes (Galand *et al.* 2009b; Galand *et al.* 2010; Martiny *et al.* 2006; Pommier *et al.* 2005) and to relate microbial diversity and ecosystem properties (Andersson *et al.* 2009).

By applying a high-throughput pyrosequencing strategy, Sogin *et al.* (2006) found a remarkably high bacterial diversity in the deep-water masses of the North Atlantic and in diffuse flow hydrothermal vents. The study highlighted the existence of thousands of low-abundance populations, coined the “rare biosphere”, which accounted for most of the observed phylogenetic bacterial diversity (Sogin *et al.* 2006). The rare phylotypes are assumed to be recruited by immigration and to have extremely low loss rates from grazing and viral lysis (Pedros-Alio

2006). Conventional molecular techniques fail to detect microbial phylotypes that make up the long tail of taxon rank-distribution curves because dominant populations (comprising > 1% of the total community) mask the detection of the highly diverse, low-abundance organisms. The massively parallel pyrotag sequencing approach, however, allows for deep sequencing that can capture information about these low-abundance populations (Galand *et al.* 2009a; Palacios *et al.* 2008; Sogin *et al.* 2006).

The spatial variability of microbial diversity across habitats has not been investigated extensively (Galand *et al.* 2010; Pommier *et al.* 2007). The availability of resources, selective loss factors (grazing and viral lysis), and physical parameters such as temperature and salinity can influence microbial population structure. This is in accordance with the deterministic theory "everything is everywhere, but, the environment selects" (Baas Becking 1934) which has been debated extensively recently (de Wit & Bouvier 2006; O'Malley 2008). In contrast, stochastic neutral models of biodiversity and biogeography (Hubbel 2001; Sloan *et al.* 2006) postulate that immigration, dispersal rates, size of the habitat (*i.e.*, taxa-area relationships) (Woodcock *et al.* 2007) and ecological invariance among microbial phylotypes shape microbial community structure.

Distinct water masses characterize the hydrodynamic conditions of the ocean, most notably the major water masses driving the thermohaline ocean circulation (Tomczak & Godfrey 2003). Non-sinking free-living prokaryotes inhabiting oceanic deep waters might be trapped in these distinct water masses leading overall to water mass-specific prokaryotic community composition and activity (Agogué *et al.* 2008; Galand *et al.* 2009b; Galand *et al.* 2010; Varela *et al.* 2008a; Varela *et al.* 2008b). Hence, dispersal and immigration of free-living microbes in the ocean might be more limited than generally assumed. These physical boundary conditions of

oceanic water masses might constrain the applicability of some of the fundamental theories and models on the biogeographic distribution of microbes in the ocean.

This study aimed at describing the composition of bacterial assemblages in the North Atlantic Ocean throughout the water column by using massively parallel pyrotag sequencing to resolve the spatial distribution of bacterial richness and evenness in different water masses. We hypothesized that the bacterial communities exhibit a biogeography according to the water masses. Hence, we expected that bacterial communities collected several 1000 km apart from each other but originating from the same water mass are more similar than bacterial communities collected less than a few hundred meters apart but from different water masses. We used data from the hypervariable V6 region of the bacterial 16S rRNA gene from 45 samples collected from the main deep water masses along a 8000 km north-to-south transect in North Atlantic Ocean ranging from 60°N to 5°S.

MATERIAL AND METHODS

Study site and sampling.

Sampling was conducted during the cruises TRANSAT-1 (September 2002) and -2 (May 2003) and ARCHIMEDES-2 (November/December 2006) on board R/V *Pelagia* following the North Atlantic Deep Water (NADW) from 60°N to 5°S in the eastern basin of the Atlantic Ocean (Fig. 1). Ten stations were occupied, and samples were taken from 6 to 10 sampling depths at each station from 100m to 4500m depth. In total, 45 samples were collected for massively parallel pyrotag sequencing (Table S1).

The water masses along the eastern North Atlantic section were identified by their distinct potential temperature and salinity characteristics (Table S2, Fig. S1) (van Aken 2000a,

b). At 4000-5000m depth, the Lower Deep Water (LDW) has low salinity (34.9) and temperature (1.9 - 2.6°C) (Table S2, Fig. S1). The NEADW (North East Atlantic Deep Water) is characterized by a temperature between 2.5 and 4.1°C and a higher salinity than LDW (Table S2, Fig. S1). The core of NEADW was identifiable throughout the transect at around 2750m depth. Two types of mesopelagic waters were found in the (sub)equatorial region: the transitional and South Atlantic Central Water (tCW/SACW) exhibiting the same temperature and salinity characteristics, and the Antarctic Intermediate Water (AAIW) characterized by lower salinity and temperature than tCW/SACW (Table S2, Fig. S1). In the northernmost region of the transect, the Northern Intermediate Water (NIW) was found at 500m depth, showing the same temperature but higher salinity than AAIW. Labrador Sea Water (LSW) was clearly identifiable at depths between 1200-2100m throughout the transect (Table S2, Fig. S1). Samples from the distinct water masses were collected with 10-L NOEX (no oxygen exchanges) bottles mounted in a CTD (conductivity, temperature, depth) frame. Samples were collected from: (i) subsurface waters (lower euphotic layer, 100-150m layer), (ii) mesopelagic waters including tCW and SACW (250 – 500m layer), AAIW (750 – 900m layer) and NIW (500m), and (iii) bathypelagic waters including LSW (1200 – 2100m layer), NEADW (1750 – 4000m layer) and LDW (4000 – 5000m layer) (Table S1).

DNA extraction, pyrosequencing and identification of the bacterial phylotypes

DNA extraction. During the TRANSAT cruises, 1 L of seawater from each depth was filtered onto a 0.2 µm polycarbonate filter (Millipore) and the filters were subsequently stored at -80°C until further processing in the lab. During the ARCHIMEDES-2 cruise, 10 L of seawater from each depth was filtered through a 0.22 µm Sterivex filter GP unit (Millipore). Lysis buffer (40

mM EDTA, 50 mM Tris-HCl, 0.75 M sucrose) was then added into the Sterivex (1.8 mL) and the filters were subsequently stored at -80°C until analysis. Extraction of total DNA was performed using an UltraClean soil DNA and Mega soil DNA isolation kit (Mobio) for TRANSAT-1 & -2 and ARCHIMEDES-2 samples, respectively.

PCR amplicon library construction and pyrosequencing. The hypervariable V6 region of the 16S rRNA of bacteria was amplified from TRANSAT samples using primers 967F, 5'-gcctccctcgcgccatcag-CAACGCGAAGAACCTTACC-3' and 1046R, 5'-gccttgccagcccgctcag-CGACAGCCATGCANCACCT-3' and pyrosequenced on a Roche Genome Sequencer 20 under conditions described in Sogin e*t al.* (2006). A cocktail of five fused primers at the 5' end of the V6 region (*E. coli* positions 967- 985) and four primers at the 3' end (*E. coli* positions 1046-1028) that capture the full diversity of rRNA sequences represented in molecular databases (Huber *et al.* 2007; Sogin *et al.* 2006) amplified ARCHIMEDES-2 environmental DNA samples for pyrosequencing on a Roche Genome GS FLX system. For both the TRANSAT and ARCHIMEDES-2 we prepared amplicon libraries from at least three independent PCR cocktails to minimize the impact of potential early-round PCR errors. To minimize effects of sequencing errors, we employed a quality trimming procedure to remove low quality pyrotags and to eliminate sequences with multiple undetermined residues or mismatches to the PCR primers at the beginning of a read (Huse *et al.* 2007).

Clustering and assignment of the OTUs: identification of bacterial phylotypes.

The clustering of V6 pyrotags into Operational Taxonomic Units (OTUs) was done with the new single-linkage preclustering (SLP) algorithm to smooth sequencing errors and reduce noise, followed by primary pairwise, average linkage clustering (PW-AL) described in Huse *et*

172 *al.* (2010). The advantage of this new method is that it corrects for sequencing errors and
173 minimizes the propagation of OTUs with sequencing effort. This method provides a comparable
174 reduction in spurious OTUs as a previously published algorithm (*e.g.* PyroNoise, Qunice *et al.*
175 2009), but requires less computational expense (Huse *et al.* 2010, see also the Discussion part on
176 pyrosequencing errors). OTUs were created using clustering thresholds of 3% corresponding to
177 97% similarity.

178 We assigned taxonomic identifiers to OTUs by using the rRNA indexing algorithm
179 Global Assignment of Sequence Taxonomy (GAST) (Sogin *et al.* 2006), which compares OTUs
180 to known rRNA genes that have already been placed in a phylogenetic framework of more than
181 1,000,000 nearly full-length rRNA reference sequences (RefSSU) based on the SILVA database
182 (Pruesse *et al.* 2007). GAST methodology is freely available through the VAMPS (Visualisation
183 and Analysis of Microbial Population Structure) website
184 (http://vamps.mbl.edu/resources/faq.php#gasting). The V6 reference database (V6RefDB: high-
185 quality, full-length 16S rRNA sequences) is publically available at: http://vamps.mbl.edu.

186

187 **Accession numbers and data availability.**

188 The OTU sequences and supporting data have been submitted to the NCBI Short Read
189 Archive (http://www.ncbi.nlm.nih.gov/Traces/home/). Run IDs are SRR029056-SRR029102
190 inclusive. One run corresponds to one sample. The sequences obtained from each run are
191 downloadable from the SRA (sequence read archive) web site of NCBI. In addition, the VAMPS
192 site http://vamps.mbl.edu provides individual and edited sequences and analytical functions for
193 interrogating the data.

194

Diversity estimation and statistical analysis.

Diversity indices. The non-parametric ACE and the Chao1 richness index were calculated with the CatchAll software program (Bunge *et al.* 2010).

The Gini index of evenness (Wittebolle *et al.* 2009) was calculated on the relative abundance of all OTUs except the singletons using the ineq function in the ineq package of the software package R for subsurface, meso- and bathypelagic samples. The higher the Gini index is, the more unevenly distributed are the OTUs.

Cluster analysis. Non-metric multidimensional scaling (MDS) (Kruskal 1964a, b) was used to determine the similarity between samples. This data-reduction method shows the differences (or similarities) between samples by reducing the comparisons between samples from a multidimensional space to fewer dimensions, preferably 2 or 3. Differences between samples were calculated based on the relative abundance of (i) all the OTUs, (ii) all the OTUs except the singletons and (iii) the 1,000 most abundant OTUs. MDS analysis was also applied to (i) all the pyrotags except the singletons, (ii) the abundant pyrotags (frequency > 1% within a sample) and (iii) the rare pyrotags (frequency < 0.01% within a sample). The similarities are presented in a multidimensional space by plotting more similar samples closer together (Kruskal 1964a, b).

Analysis of similarity (ANOSIM) was used to verify the significance of the MDS clustering by testing the hypothesis that bacterial communities from the same cluster were more similar to each other than to communities in different clusters. A Bray–Curtis similarity matrix computed from the relative abundance of all OTUs except the singletons was used to generate one-way ANOSIM statistics with 999 permutations.

SIMPER analysis. Similarity percentage (SIMPER) (Clarke & Warwick 2001) was used to determine which individual sequence contributed most to the dissimilarity between water masses

(Dataset S1). The SIMPER analysis was also used to determine the percentage of similarity (i) between each station and the northernmost station of the transect (station 27, Transat-2 cruise) (Fig.1, Table S1) within specific water layers and (ii) between water layers, based on the relative abundance of all OTUs except the singletons. The data of the NEADW from Sogin *et al.* (2006) were included in these analyses to allow full comparison of all the stations occupied from 60°N to 5°S, *i.e.*, a stretch of 8000 km.

Mantel analysis. The Mantel test was used to analyze the phylogenetic composition of the 1,000 most abundant OTUs and the singletons among all the samples. Mantel analysis was also used to determine the relationships between (i) bacterial assemblage structure, (ii) environmental factors and (iii) bacteria-related parameters. The three similarity matrices (Euclidian distance, n = 45) included the following variables: (i) the relative abundance of all OTUs except the singletons, (ii) temperature, salinity, concentration of inorganic nutrients (nitrite, nitrate, ammonia, silicate and phosphate), dissolved organic carbon (DOC) and nitrogen (DON), apparent oxygen utilization (AOU), latitude, longitude and depth and (iii) bacterial-related variables comprising bacterial abundance and production, percentage of high nucleic acid cells (HNA), potential respiration (measured as activity of the electron transport system), alpha- and beta-glucosidase, leucine aminopeptidase and alkaline phosphatase activity and its enzyme kinetics.

CCA analysis. A canonical correspondence analysis (CCA) was used to investigate the variations in the relative abundance of the 1,000 most abundant OTUs under the constraint of our set of environmental variables. We assumed a unimodal response of OTUs to environmental variations. Generally, nonlinear models are required for analysis of ecological data collected over a large range of habitats (Ter Braak & Verdonschot 1995). When a linear response is assumed, the percentage of explained variation is lower (redundancy analysis not shown). The null hypothesis

that the bacterial assemblage is independent of the environmental parameters was tested using constrained ordination with a Monte Carlo permutation test (499 permutations). The parameters were selected to obtain significant canonical axes ($p < 0.05$) and to maximize the percentage of variance explained. The cluster, the SIMPER and the Mantel analyses were performed with PRIMER 6.1.7 (Primer-E, Ltd) and XLSTAT Pro (2006) software. The CCA analysis was performed with the Canoco version 4.5 software (Ter Braak 1989).

Variability of the 100 most abundant OTUs per water mass

The deviation (in %) from the mean relative abundance in all the samples was calculated for the 100 most abundant OTUs for the different water masses. This deviation was calculated for each water mass and for each of the 100 most abundant OTUs as follows:

$$deviation\ (\%) = \left(\frac{\overline{X}_{WM}}{\overline{X}_{T}} \times 100 \right) \text{-} 100$$

where $\overline{X}_{WM}$ is the mean relative abundance of a OTU in a specific water mass and $\overline{X}_{T}$ is the mean relative abundance of this OTU in all the samples.

RESULTS

The sequencing effort yielded on average 18,111 ± 14,869 reads per sample, and ranged from 2,083 to 62,100 pyrotags among the 45 samples (Table 1). For all samples combined, we identified a total of 49,517 unique pyrotag sequences. The pyrotag length averaged 62.51 ± 3.47 bp, varying from 51 to 165 bp. On average, the unique V6 pyrotags (i.e., present in only one out of the 45 samples analyzed at an abundance >1) accounted for 14 ± 3% of the total number of pyrotags in each sample. On average each sample had 2,249 ± 1,529 unique bacterial sequences

representing nearly 835 ± 421 OTUs (Operational Taxonomic Units) at the 3% difference level. The non-parametric Chao1 and ACE estimate predicted an average number per sample of 1,416 ± 787 and 1,733 ± 1,220 OTUs, respectively. The rarefaction curves (Fig. S2) indicate that, despite obtaining on average more than 18,000 pyrotags and 10,700 OTUs identified as Bacteria, our sampling of bacterial richness was not complete.

To examine another aspect of diversity, the Gini's index of evenness was calculated for each OTU except the singletons (Fig. S3). Most of the OTUs were highly unevenly distributed (Gini > 0.5) comprising both abundant and rare OTUs. The OTUs from subsurface samples exhibited a higher evenness than the OTUs from meso- and bathypelagic samples, indicating that OTUs from subsurface were more equally distributed among samples than OTUs from deeper layers.

The 100 and 1,000 most abundant OTUs represented on average 80 ± 3% and 96 ± 1%, respectively, of the total OTU abundance in the individual samples with no significant difference among the different depth layers or water masses (Fig. 2). Significant differences between depth layers were only observed in the relative contribution of the 5 most abundant OTUs (Kruskal-Wallis test, $H = 7.01$, $p = 0.03$; Fig. 2) representing between 37% and 47% of total OTU abundance. The 5 most abundant OTUs and the 6 – 100 (34-39%) most abundant OTUs contributed roughly equally to the total OTU abundance (Fig. 2). The rank-frequency distribution of the 1,000 most abundant OTUs indicates that only a few OTUs are very abundant with a long tail of low-abundance OTUs (inset, Fig. 2). The rank-frequency distribution of meso- and bathypelagic communities exhibited a steeper slope (slope of 0.58 ± 0.01 and 0.57 ± 0.01, respectively) than that of subsurface (slope of 0.32 ± 0.01) OTUs (slope comparison, Student-t

285 test, $p < 0.001$ for all comparisons). The rank-frequency distributions of OTUs of meso- and
286 bathypelagic waters were not significantly different (Student-t test, $p > 0.05$).

287 Singleton OTUs (i.e., present in only one sample at an absolute abundance of 1)
288 comprised 5,567 OTUs out of the 10,780 distinct OTUs in our analysis. They represented half
289 (52%) of the total number of OTUs. However, they accounted for less than 2% of the total OTUs
290 abundance (Fig. 2) and, they were equally distributed among the water layers.

291 Non-metric Multidimensional Scaling (MDS) based on the relative abundance of all
292 OTUs except singletons was used to discriminate bacterial community composition in the
293 different water masses. Cluster analysis showed that bacterial community composition clustered
294 according to the water masses (Fig. 3). The samples separated into one cluster containing
295 bacterial communities of the subsurface zone, one cluster of the mesopelagic waters (AAIW and
296 tCW/SACW) and two deep-water clusters (NEADW and LDW) at 45% of similarity. Two
297 clusters of deep LSW and mesopelagic NIW bacterial communities were identified at the 55%
298 similarity level. The bacterial communities of bathypelagic waters were less similar to each other
299 than samples from subsurface and intermediate waters (Fig. 3). Bacterial communities from the
300 same water mass but separated by thousands of kilometers (S6 from St.A2-11 and S41 from St.
301 A2-45 belonging to subsurface; S12 from St. A2-19 and S40 from St. A2-45 belonging to
302 tCW/SACW; S42 from St. A2-50 and S17 from St. A2-25 belonging to NEADW) were more
303 similar to each other than communities separated by only a few hundred meters at individual
304 sites (S14 and S21 from St. A2-25; S7 and S10 from St. A2-19) but originating from different
305 water masses (Fig. 3, Table S1). The ANOSIM test showed that the differences between the
306 water mass clusters were significant ($p < 0.05$) except for AAIW and tCW/SACW ($p = 0.062$)
307 and for LSW and NIW ($p = 0.1$; Table S3). For this latter pairwise comparison, the R-value was

still high (R = 1), and the insignificant difference might be due to the low number of samples for each water mass (n = 3 for LSW and n = 2 for NIW) allowing only 10 permutations (Table S3). A MDS of the 1,000 most abundant OTUs versus all OTUs excluding the singletons produced the same clustering (data not shown). Including singletons in the MDS analysis, however, resulted in a lack of water mass-specificity of bacterial communities (data not shown). SIMPER analysis indicated that the differences in bacterial community composition between water masses are explained by the combination of abundant and rare OTUs (Dataset S1 in Suppl. Information).

The clustering of all pyrotags except the singletons was comparable to the clustering of all OTUs except the singletons (Fig S4a). The clustering of the rare sequences (frequency < 0.01% of total pyrotag abundance within a sample, Fig S4c) was similar to the clustering of the abundant sequences (frequency > 1% within a sample, Fig. S4b), albeit with a generally lower percentage of similarity. The matrices of the abundant and rare pyrotags were significantly related (Mantel test, $r = 0.68$, $p < 0.001$).

The similarity of the bacterial communities of the bathy- and mesopelagic waters decreased rapidly from the northernmost station at 60°N (station 27, Transat-2 cruise) to ≈ 50°N and remained fairly constant thereafter towards the equator (Fig. 4). Besides this pronounced latitudinal trend in similarity in the northern part of the North Atlantic, a pronounced stratification of the bacterial communities was detected (Fig. S5). In the northern part of the North Atlantic, the meso- and bathypelagic bacterial communities were more similar (47.4%) than in the southern part of the North Atlantic (37.7%) indicating an increasing stratification of bacterial communities with decreasing latitude (Fig. S5).

The relationship between bacterial assemblage structure (based on the relative abundance of all OTUs), environmental factors and the bacterial activity parameters was assessed by

correlating the three distance matrices with a Mantel test. The bacterial assemblage structure correlated with the environmental factors ($r = 0.57$, $p = 0.0001$) but not with bacterial activity parameters ($r = 0.06$, $p = 0.072$). The potential link of environmental factors with bacterial community structure was analyzed by the ordination technique of canonical correspondence analysis (CCA). The CCA indicated that samples clearly clustered according to the water masses (Fig. 5a). Depth and latitude emerged as highly significant explanatory variables, separating samples along the first and the second axes, respectively (Fig. 5a). When depth and latitude were removed from the analysis (Fig. 5b), O_2 concentration, temperature and DOC clearly separated subsurface and bathypelagic samples along the first axis. DON concentration and salinity appeared to be key factors for determining subsurface bacterial assemblage structure. When CCA was applied to bathypelagic samples (Fig. 5c), depth and temperature appeared to be significant explanatory variables, separating bathypelagic samples along the first axis, while DOC and O_2 concentrations separated samples along the second axis. The combination of depth, temperature, salinity, DOC and O_2 concentrations explained 67% of the total variance in the relative abundance of the 1,000 most abundant OTUs in bathypelagic samples. When potential density was used in the analysis instead of depth, the distribution of the bathypelagic samples in the CCA analysis was similar. When CCA was applied to mesopelagic samples (Fig. 5d), the O_2 concentration and AOU (apparent oxygen utilization) separated samples along the first axis, while depth and DOC concentration separated samples along the second axis. The combination of these parameters explained about 55% of the total variance in the relative abundance of the 1,000 most abundant OTUs in mesopelagic samples.

Phylogenetic affiliation of North Atlantic deep-water bacterial communities.

Among the 1,000 most abundant OTUs, *Proteobacteria* were, overall, the most abundant phylum (Fig. 6a), representing 84 ± 8% of the 1,000 most abundant OTUs. The bathypelagic zone exhibited the highest proportion of unassigned bacteria and a higher evenness than the overlying waters. *Deferribacteres* and, to a lesser extent, *Verrucomicrobia* increased in relative abundance with depth, and contributed 2.5% and 3.9%, respectively, to the bacterial abundance in the bathypelagic zone. *Chloroflexi* contributed to total bacterial abundance 5-fold more in bathypelagic zone (0.25%) than in subsurface (0.05%). In contrast, *Cyanobacteria* decreased with depth from 1.7% of total bacterial abundance in the subsurface layer to 0.2% in the bathypelagic zone (Fig. 6a).

Within *Proteobacteria*, *Alphaproteobacteria*, mostly composed of the SAR11 cluster (data not shown), was the most abundant class and accounted for 47% and 68% of the 1,000 most abundant proteobacterial OTUs in the bathypelagic and subsurface waters, respectively (Fig. 6b). As at the phylum level, the evenness increased with depth at the class level, and was higher in the bathypelagic zone than in the subsurface and mesopelagic zones. *Gamma-*, *Delta-* and *Betaproteobacteria* increased in relative abundance with depth, and represented 25%, 5% and 5%, respectively, of *Proteobacteria* in the bathypelagic waters.

Within *Gammaproteobacteria*, unassigned *Gammaproteobacteria* comprised the major fraction amounting to 83% of the total *Gammaproteobacteria* in the bathypelagic and to 91% in the subsurface waters (Fig. 6c). Also at the order level, evenness increased with depth and some groups were found to be specific to a specific water layer. For example, higher proportions of *Alteromonadales* (7%) and, to a lesser extent, *Oceanospirillales* (4%), *Enterobacteriales* (2%) and *Pseudomonadales* (1.6%) were found in the bathypelagic than in the subsurface zone (Fig. 6c). In contrast, *Chromatiales* were more restricted to subsurface (4%) than deep layers (1%).

Analysis of the taxonomic composition of the singletons revealed that they were as diverse as the abundant OTUs (Fig. 7). Most of the singletons belonged to the *Proteobacteria* (61%) but 11% were unassigned (Fig. 7a). Within *Proteobacteria*, *Alpha*- (38%) and *Gammaproteobacteria* (29%) dominated and 16% of the gammaproteobacterial OTUs remained unassigned (Fig. 7b). Overall, the phylogenetic composition of the singleton community was similar among all three water layers and similar to the bacterial assemblage structure of the 1,000 most abundant OTUs at the phylum (Mantel test, $r = 0.56$, $p = 0.001$) and the class level within the *Proteobacteria* (Mantel test, $r = 0.33$, $p = 0.001$).

The deviation (in %) from the mean relative abundance in all the samples of the 100 most abundant OTUs (accounting for 79 ± 8% of the OTUs abundance over all the water masses) was calculated for each water mass (Fig. 8). Lower abundance OTUs exhibit higher water mass specificity than the more abundant OTUs. OTUs specific for LSW included members of the SAR324 clade (belonging to the *Deltaproteobacteria*; OTU #3, Fig. 8 and Table S4) which accounted for 7% of the 100 most abundant OTUs, members of the SAR406 clade (belonging to *Fibrobacteres*, OTUs #30, 40 and 60) which showed the greatest variability observed among the 100 most abundant OTUs, members of the *Gammaproteobacteria* (OTUs #77, 89), *Gemmatimonadetes* (OTU #73) and *Actinobacteria* (OTU #86). OTUs specific for the NEADW included members of the *Alphaproteobacteria* (OTUs #11, 16, 24, 65 and 87), the *Betaproteobacteria* (OTU #23), the *Gammaproteobacteria* (OTUs #35, 41, 52, 66, 74 and 100), the *Deltaproteobacteria* (OTUs #75, 81, 91), the *Fibrobacteres* (members of the SAR406 clade, OTUs #25 and 98) and the *Verrucomicrobiales* (OTU #46) (Fig. 8 and Table S4). Members of the *Chloroflexi*-type SAR202 cluster (OTUs #39, 69) were generally specific for deep waters (NEADW and LSW). A large number of OTUs specific for mesopelagic waters were affiliated to

400 unassigned *Alphaproteobacteria* (OTUs #12, 53, 71, 83 and 90) and one OTU to the
401 *Verrucomicrobiales* phylum (OTU #20) (Fig. 8 and Table S4). Surface-specific OTUs were
402 mainly members of unassigned *Alphaproteobacteria* (OTUs #18, 32, 38, 48, 61, 70) and
403 *Gammaproteobacteria* (OTUs # 50, 67, 85) and one OTU from the *Actinobacteria* (OTU #99).
404 Members of the SAR11 clade (OTUs #1, 2, and 96) exhibited a ubiquitous distribution, albeit
405 they were relatively less abundant in deep-water masses (NEADW, core NEADW and LSW)
406 than in subsurface and mesopelagic waters (250 – 500m and AAIW) (Fig. 8 and Table S4). The
407 SAR11 clade contributed about 37% to the relative abundance of the 100 most abundant OTUs.
408
409 **DISCUSSION**
410 The pyrosequencing approach allowed a deep sampling of bacterial communities in North
411 Atlantic waters. The analyses of 45 samples, originating from 10 stations along a 8,000 km
412 north-to-south transect provide an exhaustive description of the distribution of bacterial
413 communities in the major deep-water masses of the North Atlantic.
414 We found water mass-specific clustering of bacterial communities throughout the major
415 North Atlantic water masses. These differences in the phylogenetic composition of the bacterial
416 community between water masses are not only due to the most abundant OTUs, but the less
417 abundant OTUs including the rare ones (but not the singletons) are also responsible for the water
418 mass-specificity of the bacterial community composition. This implies that the less abundant
419 bacterial populations exhibit biogeographical traits while the most abundant ones are more
420 ubiquitously distributed. Previous studies suggested that the rare biosphere should exhibit a high
421 rate of dispersal (Fenchel & Finlay 2004; Finlay 2002) and might act as a "seed-bank" of micro-
422 organisms which might become abundant in case of environmental changes (Palacios *et al.* 2008;

Pedros-Alio 2006). Kirchman *et al.* (2010), however, argued against the "seed-bank" hypothesis as rare phylotypes of the winter bacterial community remained rare also in the summer community in the Arctic Ocean. The distribution patterns observed for rare OTUs in the North Atlantic Ocean indicate that the rare bacterial biosphere contributes to the water mass-specificity of bacterial communities. Hence, the rare biosphere is most likely not maintained by stochastic immigration but appears to be a water mass property as also shown for the Arctic Ocean (Galand *et al.* 2010). A ubiquitous distribution of members of the rare bacterial biosphere, as previously suggested (Pedros-Alio 2006), was not found in the deep-waters of the Atlantic challenging the idea that "everything is everywhere" (Baas Becking 1934).

The singletons, *i.e.,* the OTUs present only once in all the samples, are included in the rare bacterial biosphere (Sogin *et al.* 2006). Before speculating on the potential ecological role of the rare bacterial biosphere and its origin, we need to address the question whether the presence of singletons generated by the pyrosequencing approach are fact or artifact. Random sequencing errors and miscalled bases could potentially be an explanation for the high number of singleton sequences (Gomez-Alvarez *et al.* 2009; Quince *et al.* 2009; Reeder & Knight 2009) and could inflate actual diversity estimates (Kunin *et al.* 2009). Increased sampling effort leads to a greater probability that OTUs from a given template will include variant sequences and therefore inflate the number of observed singletons. However, the frequency of variant sequences will be a function of the relative abundance of a unique starting template and the number of generated OTUs for the entire community. Sequences that correspond to high frequency templates are more likely to produce variants. A systematic and stringent trimming procedure was used in this study to remove low quality sequences and reads that did not represent the targeted region. This procedure results in a per-base error rate of 0.2-0.4% (Huse *et al.* 2007). Moreover, the newly

developed clustering method applied in this study removes spurious OTUs produced by pyrosequencing errors and minimizes the inflation of OTUs with sequencing effort (Huse *et al.* 2010). In our study, the singletons represent only 2% of the total OTU abundance in each depth zone of the North Atlantic. No clear clustering according to water masses was obtained when the singletons were included in the MDS analysis, while the bacterial community structure using all the OTUs except the singletons exhibits a water-mass specific clustering. As the singletons have the same phylogenetic composition as the 1,000 most abundant OTUs, some of the singletons might be artifacts resulting from noise in high-throughput pyrosequencing of the most abundant OTUs (Reeder & Knight 2009).

Biogeography of bacterial communities in the thermohaline ocean circulation of the North Atlantic

Distance, latitudinal gradients and area have been shown to influence bacterial community composition in lakes and the ocean (Fuhrman *et al.* 2008; Hewson *et al.* 2006; Reche *et al.* 2005). Recent phylogenetic surveys revealed a pronounced stratification among specific groups of planktonic Bacteria (DeLong 2005; Galand *et al.* 2010; Hewson *et al.* 2006; Kirchman *et al.* 2010; Martin-Cuadrado *et al.* 2007; Suzuki *et al.* 2004; Treusch *et al.* 2009) and Archaea (Agogué *et al.* 2008; Galand *et al.* 2009b; Garcia-Martinez & Rodriguez-Valera 2000). In our study, the similarity in bacterial community composition decreases rapidly in the meso- and bathypelagic waters from 60°N to 50°N and remains fairly stable thereafter. Moreover, the similarity in bacterial community composition between meso- and bathypelagic waters was higher in the northern than in the southern part of the transect. This reflects the large scale deep-water formation in the northern North Atlantic leading to a more uniform deep-water bacterial

community in the generally younger deep waters in the northern North Atlantic also exhibiting smaller differences in physico-chemical parameters between meso- and bathypelagic waters than further south towards the (sub)tropical Atlantic. Further south, distance was influencing bacterial community composition much less than water mass identity in the (sub)tropical Atlantic Ocean.

Analysis of the affiliation of the 100 most abundant OTUs revealed obvious water mass-specific signatures of bacterial community structure. Due to their distinct temperature and salinity characteristics, water masses might act as presumed dispersal barriers for bacterioplankton and hence, might limit immigration of bacterial phylotypes (Aristegui *et al.* 2009) from adjacent water masses. In the bathypelagic realm, depth and temperature were the main factors determining the composition of bacterial communities and discriminating samples from different water masses. Salinity, temperature and consequently density act as potential oceanographic barriers separating water masses and their inhabiting bacterial communities (Pommier *et al.* 2007) generating bio-oceanographic islands with specific signatures of bacterial community composition such as shown most pronouncedly for North East Atlantic Deep Water and Labrador Sea Water. Besides water mass identity and latitude, the specific environmental properties of the water masses, such as the concentrations of DOC and O_2, and AOU determine the bacterial community composition in the North Atlantic Ocean.

In contrast to our current perception of the deep ocean as a rather low diversity environment, bacterial community richness and evenness in the bathypelagic waters of the North Atlantic are as high and as variable as subsurface and mesopelagic waters. This observation is consistent with previous reports on bacterial diversity of the North Pacific and Atlantic (Hewson *et al.* 2006) and in the eastern Mediterranean Sea (Moeseneder *et al.* 2001) using fingerprinting techniques. This reported heterogeneity in deep bacterial assemblages contrasts the very slow

assemblage growth rates estimated to be 0.061 ± 0.008 d^{-1} in the deep Pacific (Aristegui *et al.* 2009) and deep-water movement (1.5 cm s^{-1}) (van Aken 2007). The heterogeneity in deep-water bacterial community composition has been interpreted to result from episodic input of organic matter from surface waters and patchiness (Hewson *et al.* 2006). However, it appears that microbial life in the dark ocean is likely more dependent on slowly sinking or buoyant, laterally advected suspended particles than hitherto assumed (Bochdansky *et al.* 2010) which might generate the water mass-specific biogeochemical conditions leading ultimately to water mass-specific bacterial assemblages (Baltar *et al.* 2009).

Vertical distribution of bacterial phylotypes

As found in previous studies on deep-sea bacterial diversity (DeLong *et al.* 2006; Fuhrman & Davis 1997; Lopez-Garcia *et al.* 2001; Pham *et al.* 2008), *Proteobacteria*, mostly from the alpha subdivision, dominate the bacterial community. Members of the alphaproteobacterial clade SAR11, ubiquitously present in the ocean (DeLong *et al.* 2006; Field *et al.* 1997; Giovannoni *et al.* 1990; Morris *et al.* 2002), decreased in relative abundance with depth.

The relative abundance of *Gammaproteobacteria*, however, increased with depth as reported previously for the North Atlantic (Lauro & Bartlett 2008; Sogin *et al.* 2006) and Antarctic Polar Front (Lopez-Garcia *et al.* 2001). Within *Gammaproteobacteri*a, members of the order *Alteromonadales* are abundant in bathypelagic waters. Several psychropiezophilic (cold and pressure-loving) bacterial isolates such as *Moritella sp.* PE36, *Psychromonas sp.* CNPT3 and *Shewanella sp.* KT99 are belonging to this order (DeLong *et al.* 1997; Lauro *et al.* 2007). We also found members of the *Oceanospirillales* more abundant in the bathypelagic North Atlantic

waters than in the subsurface and mesopelagic layers. Members of this order are also known to be symbionts of the deep-sea worm *Osedax sp.* (Goffredi *et al.* 2007; Rouse *et al.* 2009). *Betaproteobacteria* also increased in relative abundance with depth. OTUs affiliated to this class are closely related to endosymbionts of bivalves found at hydrothermal vents (Kimura *et al.* 2003). Their relatively high abundance in the free-living mode in bathypelagic waters, particularly in the North East Atlantic Deep Water (NEADW) might indicate their spreading from hydrothermal vents and/or seafloor as the NEADW flows mainly along the eastern slope of the mid-Atlantic ridge. Free-living *Betaproteobacteria* are common in freshwaters (Kirchman *et al.* 2005) but not abundant in the bathypelagic realm. However, metagenomic analysis from deep-sea methane vents have reported *Betaproteobacteria*-related phylotypes (Pernthaler *et al.* 2008), suggesting a potential niche for these organisms within methane-rich deep marine environments. In the North Pacific Ocean, Brown *et al.* (2009) recently reported an increasing relative abundance of *Betaproteobacteria* V9 pyrotags at 800m and 4400m depth. The bathypelagic bacterial community of the North Atlantic was also enriched in *Deltaproteobacteria*, as previously shown for the deep Arctic Ocean as well (Galand *et al.* 2010)) and for Station ALOHA in the North Pacific Subtropical Gyre (DeLong *et al.* 2006).

The comparison of the phylogenetic composition of the 1,000 most abundant OTUs reveals an increase of OTUs richness and evenness with depth. Thus, the bacterial community of the North Atlantic is more diverse in the bathypelagic realm than that at the base of the euphotic layer. The composition of the 100 most abundant OTUs indicates distinct water mass-specific OTUs, especially in deep waters. In meso- and bathypelagic waters, the *Deltaproteobacteria* were dominated by the SAR324 cluster (Wright *et al.* 1997), a typical deep-water clade (DeLong *et al.* 2006; Lopez-Garcia *et al.* 2001; Pham *et al.* 2008; Zaballos *et al.* 2006). The SAR406

cluster (Gordon & Giovannoni 1996) previously detected in various oceanic provinces (Gallagher *et al.* 2004; Pham *et al.* 2008) is another abundant clade of the deep Atlantic ocean, specific to the LSW. *Chloroflexi*-type SAR202 cluster, described as highly abundant in the bathypelagic subtropical North Atlantic (Morris *et al.* 2004; Varela *et al.* 2008a; Wright *et al.* 1997) was found to be a specific member of the NEADW.

Concluding remarks

By applying a high-throughput pyrosequencing strategy, we achieved a deep coverage of the bacterial populations in the deep-water masses of the North Atlantic. The bacterial assemblages clearly clustered according to the distinct water masses. The low abundance OTUs were as important for the observed water mass-specificity of bacterial community composition as the more abundant OTUs. Density differences separate water masses and their inhabiting bacterial communities, generating bio-oceanographic islands with specific signatures of bacterial community composition such as shown most pronouncedly for the deep waters. The deep bacterial assemblages exhibit a higher richness and evenness than bacterial assemblages at the base of the euphotic layer suggesting that the bathypelagic waters might offer a more heterogeneous environment for microbial life than hitherto assumed.

Acknowledgements

We acknowledge the help of H.M. van Aken for the characterization of the water masses, J. M. Arrieta for collecting and extracting the samples of the TRANSAT-1 cruise, M. Brink and D. de Corte for extracting the samples of ARCHIMEDES-2 cruise, F. Baltar for the dataset on ectoenzymatic activity, D.M Welch and S.M. Huse for the dataset on OTUs sequences and T.

Reinthaler for providing the parameters datasets of Transat and Archimedes cruises. The captain and crew of RV Pelagia provided excellent service at sea.

- Author contribution. G.J.H. and M.S. sampling scheme and sample analyses, H.A., D.L. and P.N. analyzed the data, G.J.H., P.N. and M.S. contributed the reagents/materials/analysis tools, H.A., D.L. and G.J.H wrote the paper.

- Funding. This research was supported by two Marie Curie Fellowships of the European Community to D.L. and H.A., by the Alfred P. Sloan Foundation's ICoMM field project, the W. M. Keck Foundation and a subcontract from the Woods Hole Center for Oceans and Human Health from the National Institutes of Health and the National Science Foundation (NIH_NIEHS 1 P50 ES012742-01 and NSF_OCE 0430724-J. Stegeman PI to M.L.S.). Shiptime was provided through grants of the Earth and Life Science Division of the Dutch Science Foundation (ALW-NWO) (TRANSAT and ARCHIMEDES projects) to G.J.H.

- Competing interests. The authors have declared that no competing interests exist.

REFERENCES

Agogué H, Brink M, Dinasquet J, Herndl GJ (2008) Major gradients in putatively nitrifying and non-nitrifying Archaea in the deep North Atlantic. *Nature*, **456**, 788-791.

Andersson AF, Riemann L, Bertilsson S (2009) Pyrosequencing reveals contrasting seasonal dynamics of taxa within Baltic Sea bacterioplankton communities. *ISME Journal*, **4**, 171-181.

Aristegui J, Gasol JM, Duarte CM, Herndl GJ (2009) Microbial oceanography of the dark ocean's pelagic realm. *Limnology and Oceanography*, **54**, 1501-1529.

Azam F, Fenchel T, Field JG, *et al.* (1983) The Ecological Role of Water-Column Microbes in the Sea. *Marine Ecology Progress Series*, **10**, 257-263.

Baas Becking LGM (1934) *Geobiologie of inleiding tot de milieukunde*, The Hague, the Netherlands.

Baltar F, Aristegui J, Gasol JM, Sintes E, Herndl GJ (2009) Evidence of prokaryotic metabolism on suspended particulate organic matter in the dark waters of the subtropical North Atlantic. *Limnology and Oceanography*, **54**, 182-193.

Bochdansky AB, van Aken HM, Herndl GJ (2010) Role of macroscopic particles in deep-sea oxygen sonsumption. *Proceedings of the National Academy of Sciences, USA*, **107**, 8287-8291.

Brown MV, Philip GK, Bunge JA, *et al.* (2009) Microbial community structure in the North Pacific ocean. *ISME Journal*, **3**, 1374-1386.

Bunge JA, Woodard L, Connolly S (2010) CatchAll: Parametric and nonparametric estimation of species richness and population size. *Manuscript in preparation*.

Clarke KR, Warwick RM (2001) Change in marine communities: an approach to statistical analysis and interpretation. In: *PRIMER-E Ldt*, Plymouth, UK.

DeLong EF (2005) Microbial community genomics in the ocean. *Nature Reviews: Microbiology*, **3**, 459-469.

DeLong EF, Franks DG, Yayanos AA (1997) Evolutionary Relationships of Cultivated Psychrophilic and Barophilic Deep-Sea Bacteria. *Applied and Environmental Microbiology*, **63**, 2105-2108.

DeLong EF, Preston CM, Mincer T, *et al.* (2006) Community genomics among stratified microbial assemblages in the ocean's interior. *Science* **311**, 496-503.

Fenchel T, Finlay BJ (2004) The ubiquity of small species: Patterns of local and global diversity. *BioScience*, **54**.

Field KG, Gordon D, Wright T, *et al.* (1997) Diversity and depth-specific distribution of SAR11 cluster rRNA genes from marine planktonic bacteria. *Applied and Environmental Microbiology*, **63**, 63-70.

Finlay BJ (2002) Global dispersal of free-living microbial eucaryote species. *Scienc,e* **296**.

Fuhrman JA, Davis AA (1997) Widespread archaea and novel bacteria from the deep sea as shown by 16S rRNA gene sequences. *Marine Ecology-Progress Series*, **150**, 275-285.

Fuhrman JA, Sleeter TD, Carlson CA, Proctor LM (1989) Dominance of bacterial biomass in the Sargasso Sea and its ecological implications. *Marine Ecology Progress Series*, **57**, 207-217.

Fuhrman JA, Steele JA, Hewson I, *et al.* (2008) A latitudinal diversity gradient in planktonic marine bacteria. *Proceedings of the National Academy of Sciences*, **105**, 7774-7778.

Galand PE, Casamayor EO, Kirchman DL, Lovejoy C (2009a) Ecology of the rare microbial biosphere of the Arctic Ocean. *Proceedings of the National Academy of Sciences, USA*, **106**, 22427-22432.

Galand PE, Casamayor EO, Kirchman DL, Potvin M, Lovejoy C (2009b) Unique archaeal assemblages in the Arctic Ocean unveiled by massively parallel tag sequencing. *ISME Journal*, **3**, 860-869.

Galand PE, Potvin M, Casamayor EO, Lovejoy C (2010) Hydrography shapes bacterial biogeography of the deep Arctic Ocean. *ISME Journal*, **4**, 564-576.

Gallagher JM, Carton MW, Eardly DF, Patching JW (2004) Spatio-temporal variability and diversity of water column prokaryotic communities in the eastern North Atlantic. *FEMS Microbiology Ecology* **47**, 249-262.

Garcia-Martinez J, Rodriguez-Valera F (2000) Microdiversity in uncultured marine prokaryotes: the SAR11 cluster and the marine Archaea of Group I. *Molecular Ecology*, **9**, 935-948.

Gilbert JA, Field D, Swift P, *et al.* (2009) The seasonal structure of microbial communities in the Western English Channel. *Environmental Microbiology*, **11**, 3132-3139.

Giovannoni SJ, Britschgi TB, Moyer CL, Field KG (1990) Genetic Diversity in Sargasso Sea Bacterioplankton. *Nature*, **345**, 60-63.

637 Goffredi SK, Johnson SB, Vrijenhoek RC (2007) Genetic Diversity and Potential Function of
638 Microbial Symbionts Associated with Newly Discovered Species of Osedax Polychaete
639 Worms. *Applied and Environmental Microbiology*, **73**, 2314-2323.
640 Gomez-Alvarez V, Teal TK, Schmidt TM (2009) Systematic artifacts in metagenomes from
641 complex microbial communities. *ISME Journal*, **11**, 1314-1317.
642 Gordon DA, Giovannoni SJ (1996) Detection of stratified microbial populations related to
643 Chlorobium and Fibrobacter species in the Atlantic and Pacific Oceans. *Applied and*
644 *Environmental Microbiology*, **62**, 1171-1177.
645 Handelsman J (2004) Metagenomics: Application of Genomics to Uncultured Microorganisms.
646 *Microbiology and Molecular Biology Reviews*, **68**, 669-685.
647 Hewson I, Steele JA, Capone DG, Fuhrman JA (2006) Remarkable heterogeneity in meso- and
648 bathypelagic bacterioplankton assemblage composition. *Limnology and. Oceanography*,
649 **51**, 1274-1283.
650 Huber JA, Mark Welch D, Morrison HG, *et al.* (2007) Microbial population structures in the
651 deep marine biosphere. *Science*, **318**, 97-100.
652 Huse SM, Dethlefsen L, Huber JA, *et al.* (2008) Exploring Microbial Diversity and Taxonomy
653 Using SSU rRNA Hypervariable Tag Sequencing. *Plos Genetics*, **4**, e10000255.
654 Huse SM, Huber JA, Morrison HG, Sogin ML, Mark Welch D (2007) Accuracy and quality of
655 massively parallel DNA pyrosequencing. *Genome Biology*, **8**, R143.
656 Huse SM, Welch DM, Morrison HG, Sogin ML (2010) Ironing out the wrinkles in the rare
657 biosphere through improved OTU clustering. *Environmental Microbiology*,
658 doi:10.1111/j.1462-2920.2010.02193.x.
659 Karl DM (2002) Nutrient dynamics in the deep blue sea. *Trends in Microbiology*, **10**, 410-418.
660 Kimura H, Higashide Y, Naganuma T (2003) Endosymbiotic microflora of the vestimentiferan
661 tubeworm (*Lamellibrachia sp.*) from a bathyal cold seep. *Marine Biotechnology*, **5**, 593-
662 603.
663 Kirchman DL, Cottrell MT, Lovejoy C (2010) The structure of bacterial communities in the
664 western Arctic Ocean as revealed by pyrosequencing of 16S rRNA genes. *Environmental*
665 *Microbiology*, **12**, 1132-1143.
666 Kirchman DL, Dittel AI, Malmstrom RR, Cottrell MT (2005) Biogeography of major bacterial
667 groups in the Delaware Estuary. *Limnology and Oceanography*, **50**, 1697-1706.
668 Kruskal JB (1964a) Multidimensional-Scaling by optimizing goodness of fit to a nonmetric
669 hypothesis. *Psychometrika*, **29**, 1-27.
670 Kruskal JB (1964b) Nonmetric Multidimensional Scaling - a numerical method. *Psychometrika*,
671 **29**, 115-129.
672 Kunin V, Engelbrekton A, Ochman H, Hugenholtz P (2009) Wrinkles in the rare biosphere:
673 pyrosequencing errors lead to artificial inflation of diversity estimates. *Environmental*
674 *Microbiology*, **1**, 118-123.
675 Lauro FM, Bartlett DH (2008) Prokaryotic lifestyles in deep sea habitats. *Extremophiles*, **12**, 15-
676 25.
677 Lauro FM, Chastain RA, Blankenship LE, Yayanos AA, Bartlett DH (2007) The Unique 16S
678 rRNA Genes of Piezophiles Reflect both Phylogeny and Adaptation. *Applied and*
679 *Environmental Microbiology*, **73**, 838-845.
680 Lopez-Garcia P, Lopez-Lopez A, Moreira D, Rodriguez-Valera F (2001) Diversity of free-living
681 prokaryotes from a deep-sea site at the Antarctic Polar Front. *Fems Microbiology*
682 *Ecology*, **36**, 193-202.

683 Margulies M, Egholm M, Altman WE, *et al.* (2005) Genome sequencing in microfabricated
684 high-density picolitre reactors. *Nature,* **437**, 376-380.
685 Martin-Cuadrado A-B, Lopez-Garcia P, Alba J-C, *et al.* (2007) Metagenomics of the Deep
686 Mediterranean, a Warm Bathypelagic Habitat. *PLoS ONE,* **2**, e914.
687 Martiny JBH, Bohannan BJM, Brown JH, *et al.* (2006) Microbial biogeography: putting
688 microorganisms on the map. *Nature Reviews: Microbiology,* **4**, 102-112.
689 Moeseneder MM, Winter C, Arrieta JM, Herndl GJ (2001) Terminal-restriction fragment length
690 polymorphism (T-RFLP) screening of a marine archaeal clone library to determine the
691 different phylotypes. *Journal of Microbiol Methods*, **44**, 159-172.
692 Morris RM, Rappe MS, Connon SA, *et al.* (2002) SAR11 clade dominates ocean surface
693 bacterioplankton communities. *Nature,* **420**, 806-810.
694 Morris RM, Rappe MS, Urbach E, Connon SA, Giovannoni SJ (2004) Prevalence of the
695 Chloroflexi-Related SAR202 Bacterioplankton Cluster throughout the Mesopelagic Zone
696 and Deep Ocean. *Applied and Environmental Microbiology,* **70**, 2836-2842.
697 Olsen GJ, Lane DJ, Giovannoni SJ, Pace NR, Stahl DA (1986) Microbial Ecology and
698 Evolution: A Ribosomal RNA Approach. *Annual Review of Microbiology*, **40**, 337-365.
699 Palacios C, Zettler E, Amils R, Amaral-Zettler L (2008) Contrasting microbial community
700 assembly hypotheses: a reconciling tale from the Rio Tinto. *PLoS One,* **3**, e3853.
701 Pedros-Alio C (2006) Marine microbial diversity: can it be determined? *Trends in Microbiology,*
702 **14**, 257-263.
703 Pernthaler A, Dekas AE, Brown CT, *et al.* (2008) Diverse syntrophic partnerships from deep-sea
704 methane vents revealed by direct cell capture and metagenomics. *Proceedings of the*
705 *National Academy of Sciences, USA,* **105**, 7052-7057.
706 Pham VD, Konstantinidis KT, Palden T, DeLong EF (2008) Phylogenetic analyses of ribosomal
707 DNA-containing bacterioplankton genome fragments from a 4000 m vertical profile in
708 the North Pacific Subtropical Gyre. *Environmental Microbiology,* **10**, 2313-2330.
709 Pommier T, Canback B, Riemann L, *et al.* (2007) Global patterns of diversity and community
710 structure in marine bacterioplankton. *Molecular Ecology,* **16**, 867-880.
711 Pommier T, Pinhassi J, Hagstrom A (2005) Biogeographic analysis of ribosomal RNA clusters
712 from marine bacterioplankton. *Aquatic Microbial Ecology*, **41**, 79-89.
713 Quince C, Lanzen A, Curtis TP, *et al.* (2009) Accurate determination of microbial diversity from
714 454 pyrosequencing data. *Nature Methods,* **6**, 639-641.
715 Reche I, Pulido-Villena E, Morales-Baquero R, Casamayor EO (2005) Does ecosystem size
716 determine aquatic bacterial richness? *Ecology,* **86**, 1715-1722.
717 Reeder J, Knight R (2009) The 'rare biosphere': a reality check. *Nature Methods,* **6**, 636-637.
718 Rouse G, Wilson N, Goffredi S, *et al.* (2009) Spawning and development in Osedax boneworms
719 (Siboglinidae, Annelida). *Marine Biology,* **156**, 395-405.
720 Sloan WT, Lunn M, Woodcock S, *et al.* (2006) Quantifying the roles of immigration and chance
721 in shaping prokaryote community structure. *Environmental Microbiology*, **8**, 732-740.
722 Sogin ML, Morrison HG, Huber JA, *et al.* (2006) Microbial diversity in the deep sea and the
723 underexplored "rare biosphere". *Proceedings of the National Academy of Sciences, USA,*
724 **103**, 12115-12120.
725 Suzuki MT, Preston CM, Beja O, *et al.* (2004) Phylogenetic screening of ribosomal RNA gene-
726 containing clones in bacterial artificial chromosome (BAC) libraries from different
727 depths in Monterey Bay. *Microbial Ecology*, **48**, 473-488.

Ter Braak CJ, Verdonschot PF (1995) Canonical correspondence analysis and related multivariate methods in aquatic ecology. *Aquatic Sciences*, **57**, 255-289.
Ter Braak CJF (1989) CANOCO - an extension of DECORANA to analyze species-environment relationships. *Hydrobiologia*, **184**, 169-170.
Tomczak M, Godfrey JS (2003) *Regional Oceanography: An Introduction*, 2nd edn. Daya Publishing House, Delhi.
Treusch AH, Vergin KL, Finlay LA, *et al.* (2009) Seasonality and vertical structure of microbial communities in an ocean gyre. *ISME Journal*, **3**, 1148-1163.
van Aken HM (2000a) The hydrography of the mid-latitude northeast Atlantic Ocean: I: The deep water masses. *Deep Sea Research Part I*, **47**, 757-788.
van Aken HM (2000b) The hydrography of the mid-latitude Northeast Atlantic Ocean: II: The intermediate water masses. *Deep Sea Research Part I*, **47**, 789-824.
van Aken HM (2007) *The oceanic thermohaline circulation*, Springer, New York.
Varela MM, van Aken HM, Herndl GJ (2008a) Abundance and activity of Chloroflexi-type SAR202 bacterioplankton in the meso- and bathypelagic waters of the (sub)tropical Atlantic. *Environmental Microbiology*, **10**, 1903-1911.
Varela MM, van Aken HM, Sintes E, Herndl GJ (2008b) Latitudinal trends of Crenarchaeota and Bacteria in the meso- and bathypelagic water masses of the Eastern North Atlantic. *Environmental Microbiology*, **10**, 110-124.
Wittebolle L, Marzorati M, Clement L, *et al.* (2009) Initial community evenness favours functionality under selective stress. *Nature*, **458**, 623-626.
Wright TD, Vergin KL, Boyd PW, Giovannoni SJ (1997) A novel delta-subdivision proteobacterial lineage from the lower ocean surface layer. *Applied and Environmental Microbiology*, **63**, 1441-1448.
Zaballos M, Lopez-Lopez A, Ovreas L, *et al.* (2006) Comparison of prokaryotic diversity at offshore oceanic locations reveals a different microbiota in the Mediterranean Sea. *FEMS Microbiology Ecology*, **56**, 389-405.

Figure captions

Figure 1. Location of the stations where samples for pyrosequencing were taken during the Transat-1, Transat-2 and Archimedes-2 cruises in the North Atlantic. Characteristics of the samples are given in Table S1.

Figure 2. Depth distribution of the 5, 6 – 100 and 101 – 1,000 most abundant OTUs and the singletons. Inset: Rank-frequency distribution of the 1,000 most abundant OTUs.

Figure 3. Non-metric multidimensional analysis based on relative abundance of all OTUs except the singletons. Individual samples were affiliated to their respective water-mass. Superimposed circles represent clusters of samples at similarity values of 45 and 55% (Bray-Curtis similarity). Characteristics of the samples are indicated in Table S1. The final solution was based on 25 iterations with a final stress of 0.12.

Figure 4. Similarity in relative abundance of all OTUs except the singletons (in %, calculated through SIMPER analysis) between each station and the northernmost station of the transect (station 27, Transat-2) within bathy- and mesopelagic water layers.

Figure 5. Canonical correspondence analysis of the relative abundance of the 1,000 most abundant OTUs (a) for all samples, (b) for all samples without depth and latitude as explanatory variables, (c) for bathypelagic samples and (d) for mesopelagic samples. Monte Carlo permutation tests for the first and all axes were highly significant for all the four CCA analyses ($p < 0.002$). Abbreviations of the environmental and bacteria-related variables: lat, latitude; O_2, oxygen concentration; AOU, apparent oxygen utilization; DOC, dissolved organic carbon; DON, dissolved organic nitrogen; Sal, salinity; NH_4, ammonium concentration.

Figure 6. Relative abundance and affiliation of the 1000 most abundant bacterial OTUs of each zone of the Atlantic Ocean (subsurface n=6, mesopelagic n=20 and bathypelagic n=19). (a) on

779 the phylum level, (b) the class level within *Proteobacteria*, (c) the order level within
780 *Gammaproteobacteria*.
781 **Figure 7.** Relative abundance and affiliation of the singletons of each zone of the Atlantic Ocean
782 (subsurface n=6, mesopelagic n=20 and bathypelagic n=19). (a) on the phylum level, and (b) the
783 class level within *Proteobacteria*.
784 **Figure 8**. Deviation (in %) from the mean relative abundance of the 100 most abundant OTUs
785 for all the samples for the different water masses.
786

Tables

Table 1. Sequencing information and diversity estimates for the 45 samples of the North Atlantic Ocean obtained by pyrosequencing.

	Average per sample	**Standard deviation**	**Range**
Pyrotag length (bp)	62.51	± 3.47	51 - 165
Total number of pyrotags	18111	± 14869	2083 - 62100
Total unique pyrotags	2249	± 1529	479 - 7241
% of total unique pyrotags	14	± 3	6 - 23
Total OTUs at 3% difference	835	± 421	245 - 2063
Chao1 estimator of richness at 3% difference	1416	± 787	431 - 4032
ACE estimator of richness at 3% difference	1733	± 1220	552 - 7453

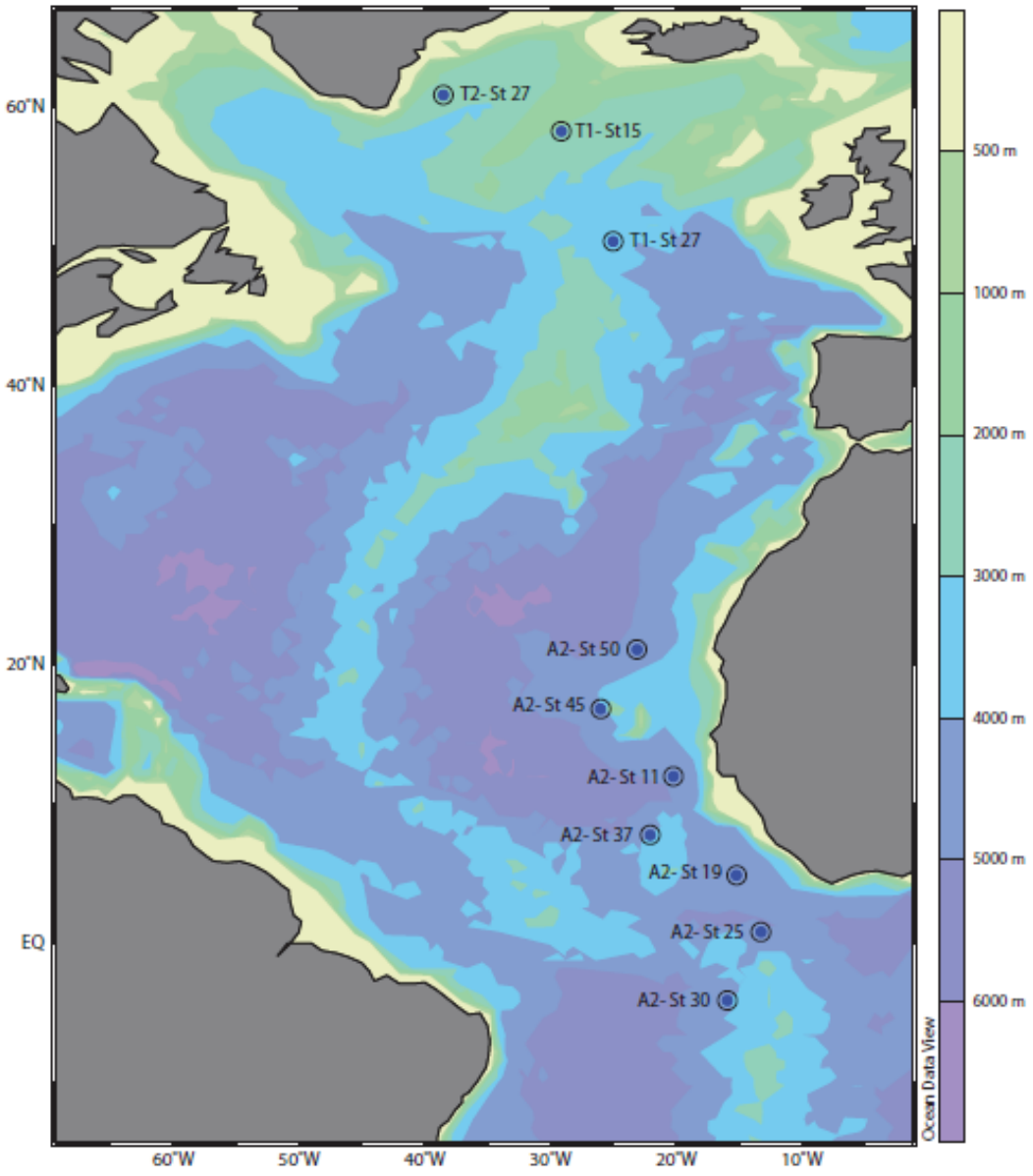
T2- St 27
T1- St15
T1- St 27
A2- St 50
A2- St 45
A2- St 11
A2- St 37
A2- St 19
A2- St 25
A2- St 30
60°N
40°N
20°N
EQ
60°W
50°W
40°W
30°W
20°W
10°W
500 m
1000 m
2000 m
3000 m
4000 m
5000 m
6000 m
Ocean Data View

Figure 1.

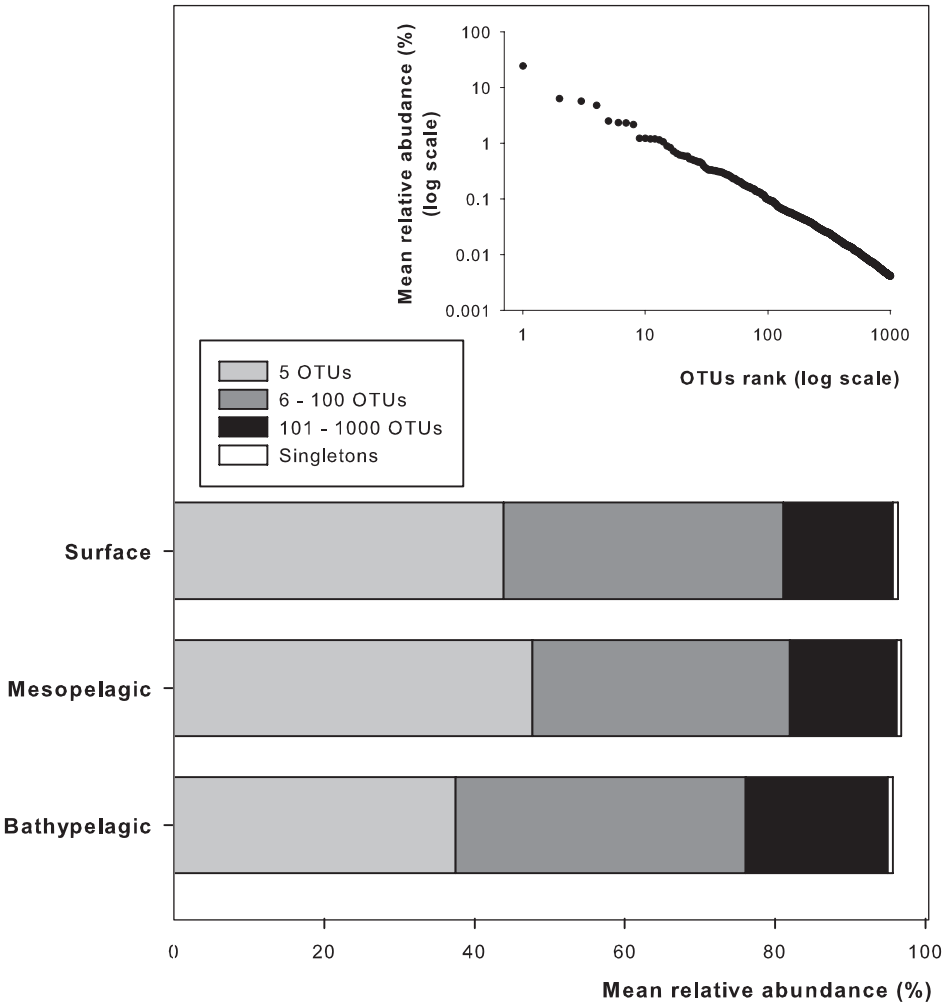
Mean relative abudance (%)
(log scale)
100
10
1
0.1
0.01
0.001
1
10
100
1000
OTUs rank (log scale)
5 OTUs
6 - 100 OTUs
101 - 1000 OTUs
Singletons
Surface
Mesopelagic
Bathypelagic
0
20
40
60
80
100
Mean relative abundance (%)

Figure 2.

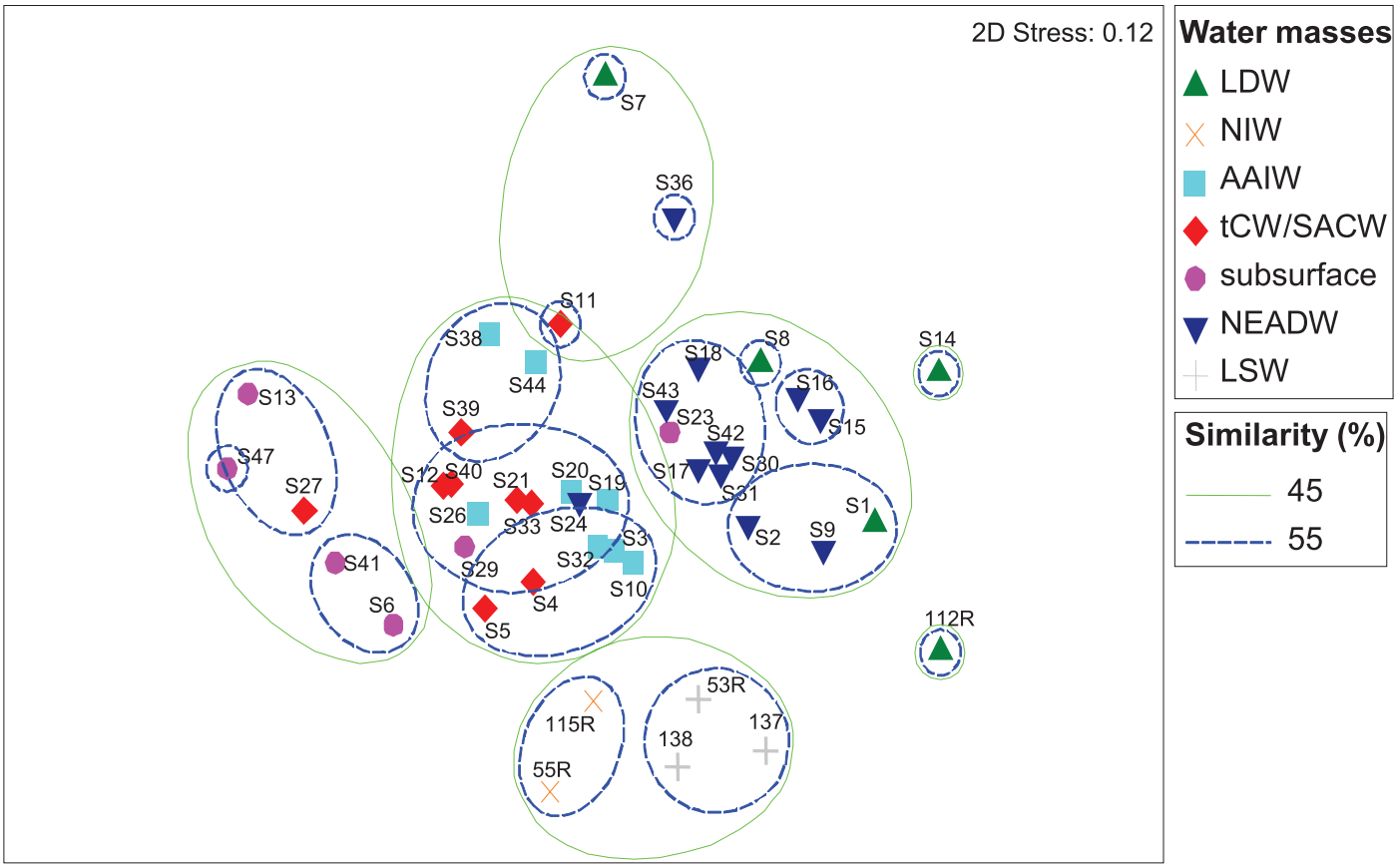
2D Stress: 0.12
Water masses
LDW
NIW
AAIW
tCW/SACW
subsurface
NEADW
LSW
Similarity (%)
45
55
S7
S36
S11
S38
S44
S8
S18
S14
S16
S43
S23
S15
S42
S39
S13
S47
S27
S12
S40
S21
S20
S19
S17
S30
S31
S1
S26
S33
S24
S2
S9
S3
S41
S29
S32
S10
S6
S4
S5
112R
53R
115R
137
138
55R

Figure 3.

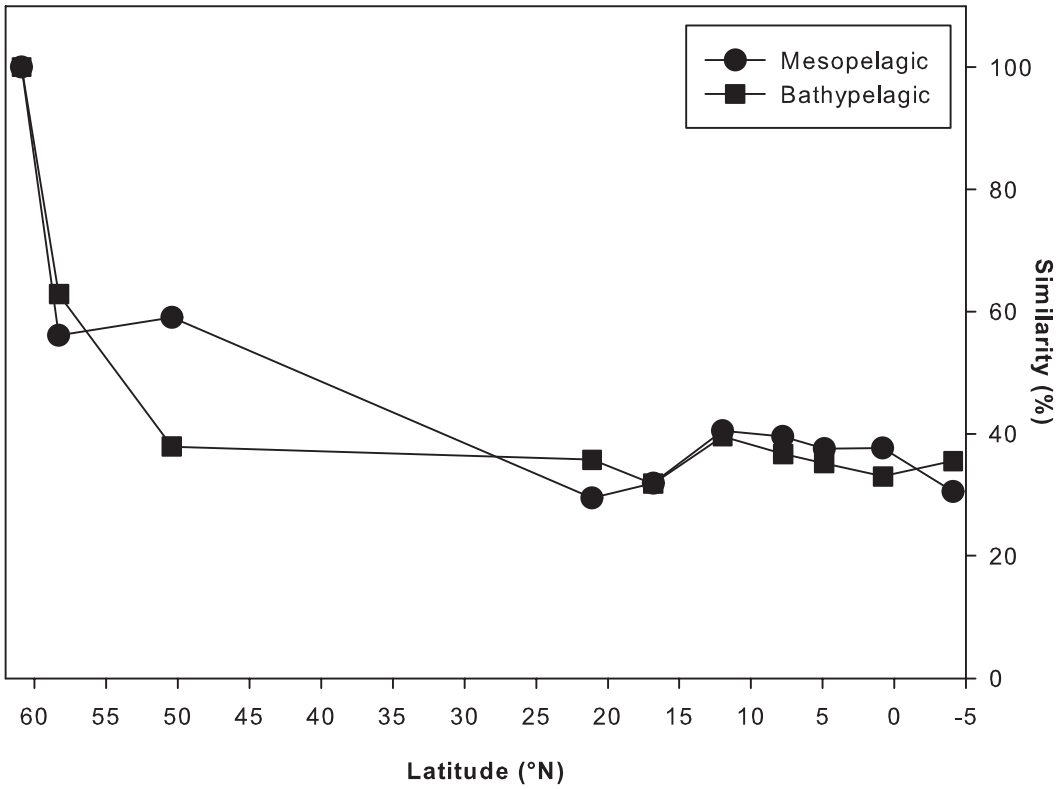
Mesopelagic
Bathypelagic
100
80
60
40
20
0
Similarity (%)
60
55
50
45
40
35
30
25
20
15
10
5
0
-5
Latitude (°N)

Figure 4.

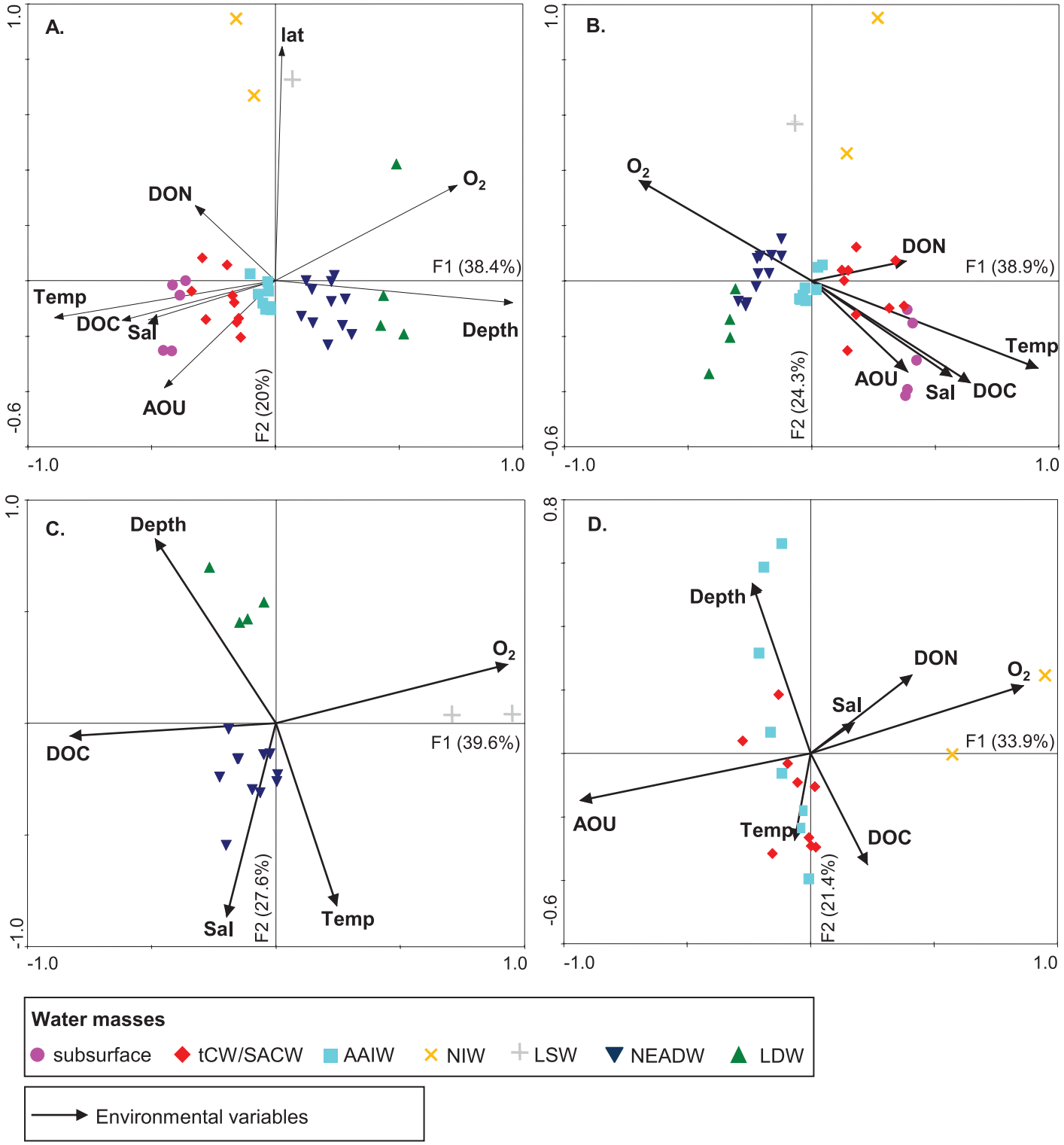
A.
lat
DON
O2
F1 (38.4%)
Temp
DOC
Sal
Depth
AOU
F2 (20%)
1.0
-0.6
-1.0
1.0
B.
O2
DON
F1 (38.9%)
Temp
AOU
Sal
DOC
F2 (24.3%)
C.
Depth
O2
DOC
F1 (39.6%)
Sal
Temp
F2 (27.6%)
D.
Depth
DON
O2
Sal
F1 (33.9%)
AOU
Temp
DOC
F2 (21.4%)
0.8
Water masses
subsurface
tCW/SACW
AAIW
NIW
LSW
NEADW
LDW
Environmental variables

Figure 5.

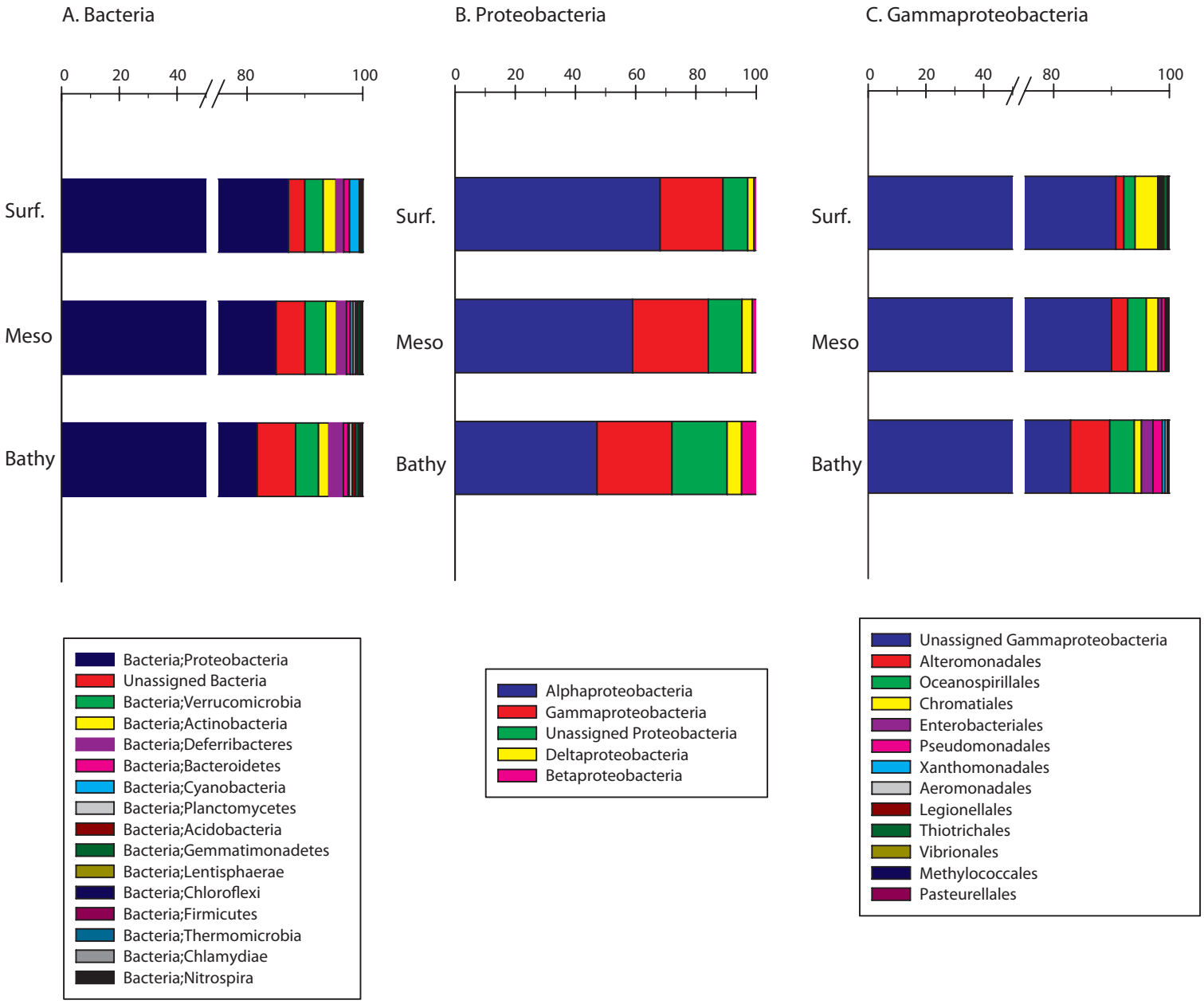
A. Bacteria
B. Proteobacteria
C. Gammaproteobacteria
0
20
40
80
100
60
Surf.
Meso
Bathy
Bacteria;Proteobacteria
Unassigned Bacteria
Bacteria;Verrucomicrobia
Bacteria;Actinobacteria
Bacteria;Deferribacteres
Bacteria;Bacteroidetes
Bacteria;Cyanobacteria
Bacteria;Planctomycetes
Bacteria;Acidobacteria
Bacteria;Gemmatimonadetes
Bacteria;Lentisphaerae
Bacteria;Chloroflexi
Bacteria;Firmicutes
Bacteria;Thermomicrobia
Bacteria;Chlamydiae
Bacteria;Nitrospira
Alphaproteobacteria
Gammaproteobacteria
Unassigned Proteobacteria
Deltaproteobacteria
Betaproteobacteria
Unassigned Gammaproteobacteria
Alteromonadales
Oceanospirillales
Chromatiales
Enterobacteriales
Pseudomonadales
Xanthomonadales
Aeromonadales
Legionellales
Thiotrichales
Vibrionales
Methylococcales
Pasteurellales

Figure 6.

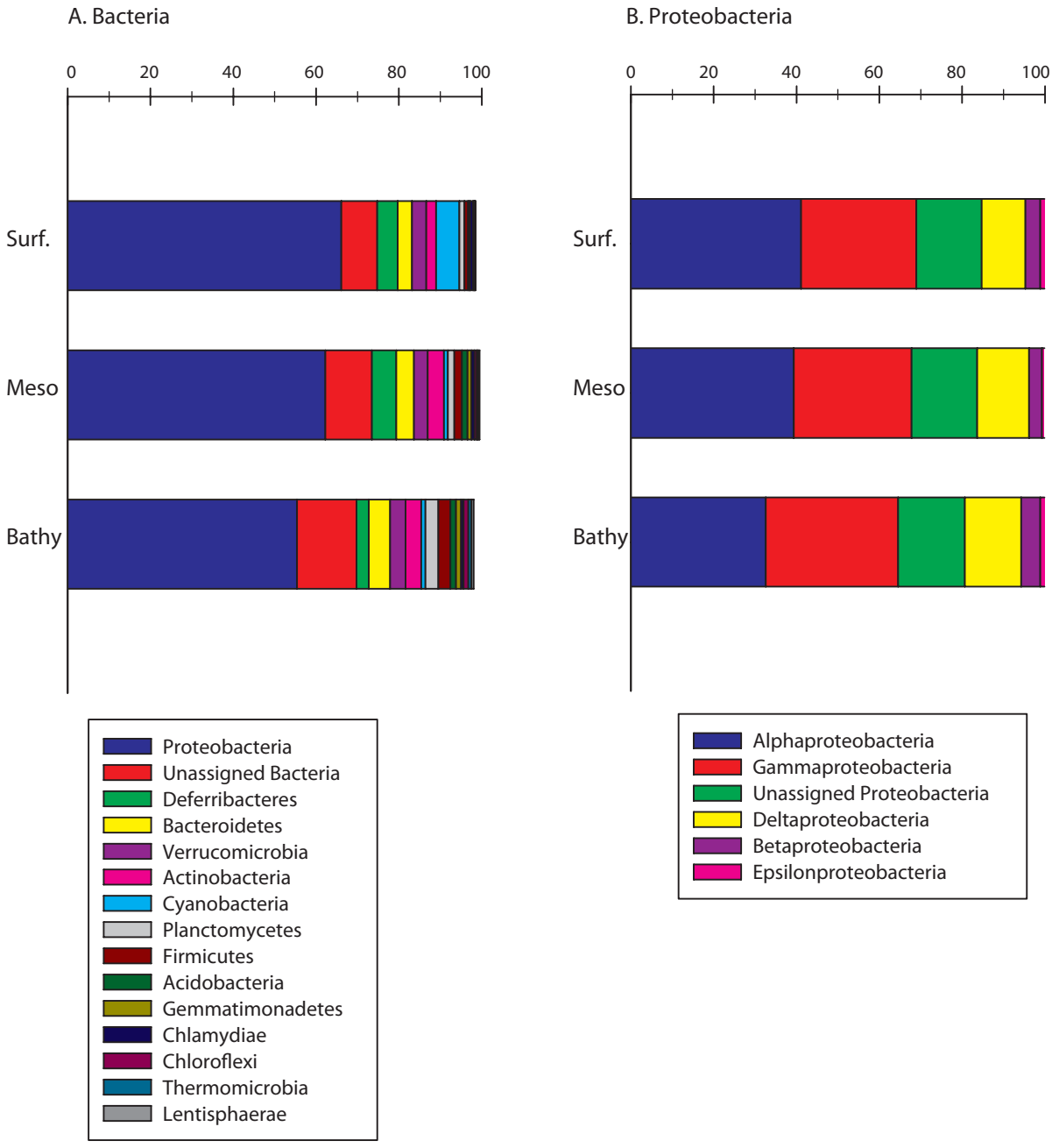
A. Bacteria
0
20
40
60
80
100
Surf.
Meso
Bathy
Proteobacteria
Unassigned Bacteria
Deferribacteres
Bacteroidetes
Verrucomicrobia
Actinobacteria
Cyanobacteria
Planctomycetes
Firmicutes
Acidobacteria
Gemmatimonadetes
Chlamydiae
Chloroflexi
Thermomicrobia
Lentisphaerae
B. Proteobacteria
0
20
40
60
80
100
Surf.
Meso
Bathy
Alphaproteobacteria
Gammaproteobacteria
Unassigned Proteobacteria
Deltaproteobacteria
Betaproteobacteria
Epsilonproteobacteria

Figure 7.

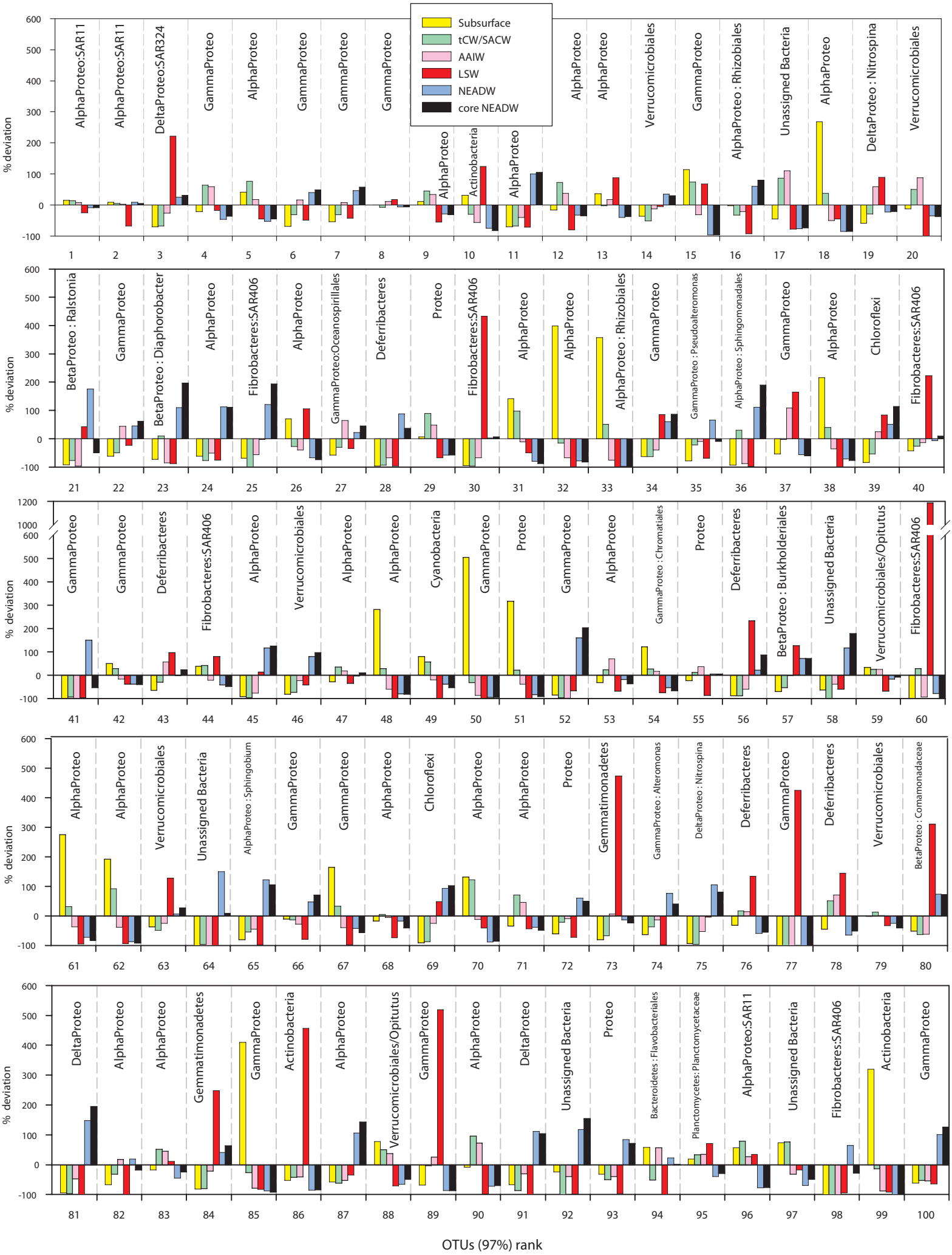
Subsurface
tCW/SACW
AAIW
LSW
NEADW
core NEADW
% deviation
OTUs (97%) rank

Figure 8.

Supplementary methods.

Environmental parameters

Inorganic nutrients — The methods for determining inorganic nutrient concentrations followed Joint Global Ocean Fluxes Study recommendations (Gordon *et al.* 1993). The concentrations of dissolved inorganic nutrients (NH_4^+ , NO_3^- , NO_2^-, PO_4^{3-}) were determined in a TRAACS autoanalyzer immediately after collecting the samples and gentle filtration through 0.2 µm filters (Acrodisc, Gelman Science). NH_4^+ was detected with the indophenol blue method (pH 10.5) at 630 nm. NO_2^- was detected after diazotation with sulfanilamide and *N*-(1-naphtyl)-ethylene diammonium dichloride as the reddishpurple dye complex at 540 nm. NO_3^- was reduced in a copper cadmium coil to nitrite (with imidazole as a buffer) and then measured as nitrite. Inorganic PO_4^{3-} was determined via the molybdenum blue complex at 880 nm.

Dissolved organic carbon (DOC) — Samples for DOC were filtered through rinsed 0.2 µm polycarbonate filters and sealed in precombusted (450°C for 4 h) glass ampoules after adding 50 µL of 40% phosphoric acid. The samples were stored frozen at -20°C until analysis back in the lab. DOC concentrations of duplicate samples were determined using a Shimadzu TOC-5000 analyzer. Three-point standard curves, prepared with potassium hydrogen phthalate (Nacalai Tesque, Kyoto, Japan), were used to calculate DOC concentrations. The instrument's performance and the validity of the calibration were determined using reference material of the Hansell CRM program (44–46 µmol L^{-1} for the reference samples; n = 3 and 1–2 µmol L^{-1} for low carbon water; n = 3). The average analytical precision of the instrument was < 3%.

Dissolved organic nitrogen (DON) — Total dissolved nitrogen (TDN) was analyzed with a TRAACS 800 continuous-flow analysis system following the persulfate oxidation method. DON concentrations were calculated by subtracting the sum of the inorganic nitrogen species from

TDN concentrations. The recovery of DON was estimated on a mixture of 10 different organic compounds containing known concentrations of N (Kramer *et al.* 2005). For this reference material, the recovery efficiency of organic nitrogen was 92% of the calculated organic nitrogen concentration.

Bacterial-related parameters

Prokaryotic abundance determined by flow cytometry — Prokaryotic plankton collected from the different depth layers of the water column were enumerated using flow cytometry. Samples (2 ml) were fixed with 1% paraformaldehyde (final concentration), shock-frozen in liquid nitrogen for 5 min and stored at -80°C (Kamiya *et al.* 2007). Picoplankton cells were stained with SYBR-Green I and enumerated with a FACSCalibur flow cytometer (BectonDickinson) within 2 months. Immediately before analysis, the thawed picoplankton samples were stained with SYBRGreen I at room temperature in the dark for 15 min. Fluorescent microspheres (Molecular Probes) with a diameter of 1 mm were added to all samples as an internal standard. Counts were performed with an argon laser at 488 nm wavelength. Prokaryotic cells were enumerated according to their right angle scatter and green fluorescence. The counting window of the flow cytometer was set to exclude eukaryotic picoplankton.

Prokaryotic heterotrophic production by [^{3}H] leucine incorporation — Bulk PHP was measured by incubating triplicate 10–40 ml samples and formaldehyde-killed blanks (2% final concentration) with 10 nM [^{3}H]-leucine (final concentration, specific activity 160 Ci mmol^{-1}; Amersham) in temperature-controlled incubators in the dark at *in situ* temperature for 4–10 h (Kirchman *et al.* 1985). Incubations were terminated by adding formaldehyde (2% final concentration) before filtering the samples and the blanks through 0.2 µm polycarbonate filters (25 mm filter diameter; Millipore). Subsequently, the filters were rinsed three times with 5% ice-

cold trichloroacetic acid, dried and placed in scintillation vials. Scintillation cocktail (8 ml Canberra-Packard Filter Count) was added, and after 18 h, counted in a liquid scintillation counter (LKB Wallac model 1212). The mean disintegrations per minute (DPM) of the formaldehyde-fixed blanks were subtracted from the mean DPM of the respective samples, and the resulting DPM converted into leucine incorporation rates. Prokaryotic carbon biomass production was estimated using a conservative theoretical conversion factor of 1.55 kg C mol^{-1} Leu assuming no internal isotope dilution (Kirchman & Ducklow 1993).

Activity of the ETS — Electron transport system (ETS) activity was measured following the modifications of the tetrazolium reduction technique as described earlier (Aristegui & Montero 1995). Some minor modifications of the method were made to increase its sensitivity (Baltar *et al.* 2009).

Measurements of prokaryotic extracellular enzymatic activity — The hydrolysis of the fluorogenic substrate analogues 4-methylcoumarinyl-7-amide (MCA)-L-leucine-7-amido-4-methylcoumarin, 4-methylumbelliferyl (MUF)-a-D-glucoside, 4-MUF-b-D-glucoside and MUF-phosphate was measured to estimate potential activity rates of alpha-, beta-glucosidase, aminopeptidase and alkaline phosphatase, respectively (Baltar *et al.* 2009; Hoppe 1983).

The environmental data used in statistical analysis can be found at: http://icomm.mbl.edu/microbis.

References

Aristegui J, Montero MF (1995) The relationship between community respiration and ETS activity in the ocean. *Journal of Plankton Research* **17**, 1563-1571.

Baltar F, Aristegui J, Gasol JM, Sintes E, Herndl GJ (2009) Evidence of prokaryotic metabolism on suspended particulate organic matter in the dark waters of the subtropical North Atlantic. *Limnology and Oceanography* **54**, 182-193.

Gordon LI, Jennings J, Ross AA, Krest JM (1993) A suggested protocol for continuous flow automated analysis of seawater nutrients (phosphate, nitrate, nitrite and silicic acid) in the WOCE Hydrographic Program and the Joint Global Ocean Fluxes Study. In: *WOCE Operation manual, WHP Operations and Methods*, p. 52. WOCE Hydrographic Program Office.

Hoppe H-G (1983) Significance of exoenzymatic activities in the ecology of brackish water: measurements by means of methylumbelliferyl-subtrates. *Marine Ecology Progress Series* **11**, 299-308.

Kamiya E, Izumiyama S, Nishimura M, Mitchell J, Kogure K (2007) Effects of fixation and storage on flow cytometric analysis of marine bacteria. *Journal of Oceanography* **63**, 101-112.

Kirchman DL, Ducklow HW (1993) Estimating converting factors for thymidine and leucine methods for measuring bacterial production. In: *Handbook of methods in aquatic microbial ecology* (eds. Kemp PF, Sherr BF, Sherr EB, Cole JJ), pp. 513-517. Lewis, Boca Raton.

Kirchman DL, K'Ness E, Hodson R (1985) Leucine incorporation and its potential as a mesure of protein synthesis by bacteria in natural aquatic systems. *Applied and Environmental Microbiology* **49**, 599-607.

Kramer GD, Pausz C, Herndl GJ (2005) Elemental composition of dissolved organic matter and bacterioplankton production in the Faroe-Shetland Channel (North Atlantic). *Deep-Sea Research Part I Oceanographic Research Papers* **52**, 85-97.

Table S1. Description of the 45 samples from the North Atlantic Ocean selected for bacterial pyrosequencing. LDW: Lower Deep Water, NEADW: North East Atlantic Deep Water, AAIW: Antarctic Intermediate Water, tCW/SACW: transitional/South Atlantic Central Water, NIW: Northern Intermediate Water, LSW: Labrador Sea Water).

Sample ID	Cruise	Station	Longitude °E	Latitude °N	Depth (m)	Water mass
53R	Transat-1	15	-29.13	58.3	1400	LSW
55R	Transat-1	15	-29.13	58.3	500	NIW
112R	Transat-1	27	-25	50.4	4000	LDW
115R	Transat-1	27	-25	50.4	500	NIW
137	Transat-2	27	-38.52	60.9	1700	LSW
138	Transat-2	27	-38.52	60.9	700	LSW
S1	Archimedes-2	11	-20.21	11.98	4000	LDW
S2	Archimedes-2	11	-20.21	11.98	2750	NEADW
S3	Archimedes-2	11	-20.21	11.98	900	AAIW
S4	Archimedes-2	11	-20.21	11.98	500	tCW
S5	Archimedes-2	11	-20.21	11.98	250	tCW
S6	Archimedes-2	11	-20.21	11.98	100	Subsurface
S7	Archimedes-2	19	-15.19	4.9	4500	LDW
S8	Archimedes-2	19	-15.19	4.9	4000	LDW
S9	Archimedes-2	19	-15.19	4.9	2750	NEADW
S10	Archimedes-2	19	-15.19	4.9	900	AAIW
S11	Archimedes-2	19	-15.19	4.9	500	SACW
S12	Archimedes-2	19	-15.19	4.9	250	SACW
S13	Archimedes-2	19	-15.19	4.9	100	Subsurface
S14	Archimedes-2	25	-13.24	0.81	4500	LDW
S15	Archimedes-2	25	-13.24	0.81	3500	NEADW
S16	Archimedes-2	25	-13.24	0.81	3000	NEADW
S17	Archimedes-2	25	-13.24	0.81	2000	NEADW
S18	Archimedes-2	25	-13.24	0.81	1800	NEADW
S19	Archimedes-2	25	-13.24	0.81	900	AAIW
S20	Archimedes-2	25	-13.24	0.81	750	AAIW
S21	Archimedes-2	25	-13.24	0.81	500	SACW
S23	Archimedes-2	25	-13.24	0.81	100	Subsurface
S24	Archimedes-2	30	-13.24	0.81	2500	NEADW
S26	Archimedes-2	30	-15.91	-4.09	750	AAIW
S27	Archimedes-2	30	-15.91	-4.09	500	tCW
S29	Archimedes-2	30	-15.91	-4.09	100	Subsurface
S30	Archimedes-2	37	-22.05	7.78	2500	NEADW
S31	Archimedes-2	37	-22.05	7.78	1800	NEADW
S32	Archimedes-2	37	-22.05	7.78	750	AAIW
S33	Archimedes-2	37	-22.05	7.78	500	tCW
S36	Archimedes-2	45	-26.0	16.83	2500	NEADW
S38	Archimedes-2	45	-26.0	16.83	900	AAIW
S39	Archimedes-2	45	-26.0	16.83	500	tCW
S40	Archimedes-2	45	-26.0	16.83	250	tCW
S41	Archimedes-2	45	-26.0	16.83	100	Subsurface
S42	Archimedes-2	50	-23.11	21.09	2500	NEADW
S43	Archimedes-2	50	-23.11	21.09	1800	NEADW
S44	Archimedes-2	50	-23.11	21.09	900	AAIW
S47	Archimedes-2	50	-23.11	21.09	100	Subsurface

Table S2. Water mass properties (depth, mean and range of potential temperature and salinity) of the different water type of the North Atlantic (tCW/SACW: transitional/South Atlantic Central Water, AAIW: Antarctic Intermediate Water, NIW: Northern Intermediate Water, LSW: Labrador Sea Water, NEADW: North East Atlantic Deep water, LDW: Lower Deep Water) and number of samples (n).

Water mass	**Depth (m)**	**Pot .Temp.* (°C)**	**Range (°C)**	**Salinity**	**Range**	**n**
Subsurface	100 - 150	16.7	14.2 – 20.6	35.97	35.45 – 37.06	6
tCW/SACW	250 - 500	9.9	7.4 – 13.2	35.05	34.66 – 35.62	9
NIW	500 - 750	7.1	7.0 – 7.1	35.09	35.05 – 35.12	2
AAIW	750 - 900	5.6	4.6 – 6.7	34.70	34.50 – 34.99	8
LSW	1200 - 2100	3.3	3.0 – 3.5	34.89	34.87 – 34.92	3
NEADW	1750 - 4000	3.0	2.2 – 4.0	34.95	34.90 – 35.03	12
LDW	4000 - 5000	1.9	1.5 – 2.3	34.88	34.84 – 34.92	5

* Pot. Temp.: potential temperature

Table S3. ANOSIM test between water masses (tCW/SACW: transitional/South Atlantic Central Water, AAIW: Antarctic Intermediate Water, NIW: Northern Intermediate Water, LSW: Labrador Sea Water, NEADW: North East Atlantic Deep water, LDW: Lower Deep Water) based on the relative abundance of all OTUs (97%) except the singletons.

Global R = 0.597; Significance level = 0.001; Number of permutations: 999

Pairwise tests between water masses	R-value	Significance level	Actual permutations
Subsurface, AAIW	0.444	0.007	999
Subsurface, tCW/SACW	0.228	0.034	999
Subsurface, NEADW	0.722	0.002	999
Subsurface, LDW	0.744	0.006	462
Subsurface, LSW	0.772	0.012	84
Subsurface, NIW	0.51	0.036	56
AAIW, tCW/SACW	0.115	0.062 (n.s.*)	999
AAIW, NEADW	0.428	0.001	999
AAIW, LDW	0.796	0.002	999
AAIW, LSW	0.874	0.006	165
AAIW, NIW	0.716	0.022	45
tCW/SACW, NEADW	0.759	0.001	999
tCW/SACW, LDW	0.878	0.001	999
tCW/SACW, LSW	0.937	0.005	220
tCW/SACW, NIW	0.709	0.018	55
NEADW, LDW	0.744	0.006	462
NEADW, LSW	0.89	0.002	455
NEADW, NIW	0.937	0.011	91
LDW, LSW	0.508	0.036	56
LDW, NIW	0.545	0.048	21
LSW, NIW	1	0.1 (n.s.*)	10

*n.s.: non-significant

Table S4. Characteristics of the 100 most abundant OTUs (# of OTUs; ID, identification number; percent of contribution to the 100 most abundant OTUs; affiliation)

# OTU	Cluster ID	% to the 100 first OTUss	Affiliation
1	Alphaproteobacteria_03_1	29,72	Bacteria;Proteobacteria;Alphaproteobacteria;Rickettsiales;SAR11
2	Alphaproteobacteria_03_2	7,87	Bacteria;Proteobacteria;Alphaproteobacteria;Rickettsiales;SAR11
3	ProteobacteriaNA_03_1	7,06	Bacteria;Proteobacteria
4	Gammaproteobacteria_03_8	5,85	Bacteria;Proteobacteria;Gammaproteobacteria
5	Alphaproteobacteria_03_21	3,08	Bacteria;Proteobacteria;Alphaproteobacteria
6	Gammaproteobacteria_03_29	2,93	Bacteria;Proteobacteria;Gammaproteobacteria
7	Gammaproteobacteria_03_47	2,88	Bacteria;Proteobacteria;Gammaproteobacteria
8	Gammaproteobacteria_03_44	2,69	Bacteria;Proteobacteria;Gammaproteobacteria
9	ProteobacteriaNA_03_6	1,52	Bacteria;Proteobacteria
10	Actinobacteria_03_4	1,54	Bacteria;Actinobacteria;Actinobacteria
11	ProteobacteriaNA_03_8	1,52	Bacteria;Proteobacteria
12	Alphaproteobacteria_03_53	1,46	Bacteria;Proteobacteria;Alphaproteobacteria
13	Alphaproteobacteria_03_26	1,41	Bacteria;Proteobacteria;Alphaproteobacteria
14	Verrucomicrobia_03_3	1,33	Bacteria;Verrucomicrobia;Verrucomicrobiae;Verrucomicrobiales
15	Gammaproteobacteria_03_52	1,11	Bacteria;Proteobacteria;Gammaproteobacteria
16	Alphaproteobacteria_03_258	1,03	Bacteria;Proteobacteria;Alphaproteobacteria;Rhizobiales
17	BacteriaNA_03_2	0,89	Bacteria
18	Alphaproteobacteria_03_20	0,81	Bacteria;Proteobacteria;Alphaproteobacteria
19	Deltaproteobacteria_03_2	0,75	Bacteria;Proteobacteria;Deltaproteobacteria;Desulfobacterales;Nitrospinaceae;Nitrospina
20	Verrucomicrobia_03_6	0,73	Bacteria;Verrucomicrobia;Verrucomicrobiae;Verrucomicrobiales
21	Betaproteobacteria_03_1	0,87	Bacteria;Proteobacteria;Betaproteobacteria;Burkholderiales;Burkholderiaceae;Ralstonia
22	Gammaproteobacteria_03_106	0,72	Bacteria;Proteobacteria;Gammaproteobacteria
23	Betaproteobacteria_03_11	0,74	Bacteria;Proteobacteria;Betaproteobacteria;Burkholderiales;Comamonadaceae;Diaphorobacter
24	ProteobacteriaNA_03_14	0,64	Bacteria;Proteobacteria
25	BacteriaNA_03_15	0,62	Bacteria
26	Alphaproteobacteria_03_17	0,60	Bacteria;Proteobacteria;Alphaproteobacteria
27	Gammaproteobacteria_03_78	0,57	Bacteria;Proteobacteria;Gammaproteobacteria;Oceanospirillales
28	Deferribacteres_03_6	0,61	Bacteria;Deferribacteres
29	ProteobacteriaNA_03_12	0,53	Bacteria;Proteobacteria
30	BacteriaNA_03_6	0,49	Bacteria
31	Alphaproteobacteria_03_94	0,45	Bacteria;Proteobacteria;Alphaproteobacteria
32	Alphaproteobacteria_03_71	0,44	Bacteria;Proteobacteria;Alphaproteobacteria
33	Alphaproteobacteria_03_261	0,40	Bacteria;Proteobacteria;Alphaproteobacteria;Rhizobiales
34	Gammaproteobacteria_03_128	0,41	Bacteria;Proteobacteria;Gammaproteobacteria
35	Gammaproteobacteria_03_7	0,41	Bacteria;Proteobacteria;Gammaproteobacteria;Alteromonadales;Pseudoalteromonadaceae;Pseudoalteromona
36	Alphaproteobacteria_03_27	0,45	Bacteria;Proteobacteria;Alphaproteobacteria;Sphingomonadales;Sphingomonadaceae
37	Gammaproteobacteria_03_113	0,39	Bacteria;Proteobacteria;Gammaproteobacteria
38	Alphaproteobacteria_03_30	0,39	Bacteria;Proteobacteria;Alphaproteobacteria
39	BacteriaNA_03_10	0,39	Bacteria
40	BacteriaNA_03_14	0,38	Bacteria
41	Gammaproteobacteria_03_19	0,43	Bacteria;Proteobacteria;Gammaproteobacteria
42	Gammaproteobacteria_03_40	0,38	Bacteria;Proteobacteria;Gammaproteobacteria
43	Deferribacteres_03_10	0,37	Bacteria;Deferribacteres
44	BacteriaNA_03_49	0,36	Bacteria
45	Alphaproteobacteria_03_116	0,36	Bacteria;Proteobacteria;Alphaproteobacteria
46	Verrucomicrobia_03_17	0,35	Bacteria;Verrucomicrobia;Verrucomicrobiae;Verrucomicrobiales;Verrucomicrobiaceae
47	Alphaproteobacteria_03_159	0,34	Bacteria;Proteobacteria;Alphaproteobacteria
48	Alphaproteobacteria_03_75	0,33	Bacteria;Proteobacteria;Alphaproteobacteria
49	Cyanobacteria_03_1	0,32	Bacteria;Cyanobacteria;True Cyanobacteria;Prochlorales

50	Gammaproteobacteria_03_130	0,31	Bacteria;Proteobacteria;Gammaproteobacteria
51	ProteobacteriaNA_03_7	0,30	Bacteria;Proteobacteria
52	Gammaproteobacteria_03_270	0,30	Bacteria;Proteobacteria;Gammaproteobacteria
53	Alphaproteobacteria_03_169	0,29	Bacteria;Proteobacteria;Alphaproteobacteria
54	Gammaproteobacteria_03_9	0,28	Bacteria;Proteobacteria;Gammaproteobacteria;Chromatiales;Ectothiorhodospiraceae
55	ProteobacteriaNA_03_22	0,28	Bacteria;Proteobacteria
56	Deferribacteres_03_11	0,27	Bacteria;Deferribacteres
57	Betaproteobacteria_03_3	0,28	Bacteria;Proteobacteria;Betaproteobacteria;Burkholderiales;Comamonadaceae
58	BacteriaNA_03_18	0,26	Bacteria
59	Verrucomicrobia_03_45	0,25	Bacteria;Verrucomicrobia;Opitutae;Opitutales;Opitutaceae;Opitutus
60	BacteriaNA_03_4	0,24	Bacteria
61	Alphaproteobacteria_03_79	0,24	Bacteria;Proteobacteria;Alphaproteobacteria
62	Alphaproteobacteria_03_52	0,23	Bacteria;Proteobacteria;Alphaproteobacteria
63	Verrucomicrobia_03_29	0,23	Bacteria;Verrucomicrobia;Verrucomicrobiae;Verrucomicrobiales
64	BacteriaNA_03_41	0,23	Bacteria
65	Alphaproteobacteria_03_18	0,24	Bacteria;Proteobacteria;Alphaproteobacteria;Sphingomonadales;Sphingomonadaceae;Sphingobium
66	Gammaproteobacteria_03_206	0,21	Bacteria;Proteobacteria;Gammaproteobacteria
67	Gammaproteobacteria_03_25	0,21	Bacteria;Proteobacteria;Gammaproteobacteria
68	Alphaproteobacteria_03_14	0,21	Bacteria;Proteobacteria;Alphaproteobacteria
69	BacteriaNA_03_35	0,21	Bacteria
70	Alphaproteobacteria_03_242	0,20	Bacteria;Proteobacteria;Alphaproteobacteria
71	Alphaproteobacteria_03_155	0,20	Bacteria;Proteobacteria;Alphaproteobacteria
72	ProteobacteriaNA_03_25	0,20	Bacteria;Proteobacteria
73	Gemmatimonadetes_03_3	0,18	Bacteria;Gemmatimonadetes
74	Gammaproteobacteria_03_15	0,19	Bacteria;Proteobacteria;Gammaproteobacteria;Alteromonadales;Alteromonadaceae;Alteromonas
75	Deltaproteobacteria_03_106	0,19	Bacteria;Proteobacteria;Deltaproteobacteria;Desulfobacterales;Nitrospinaceae;Nitrospina
76	Deferribacteres_03_7	0,19	Bacteria;Deferribacteres
77	Gammaproteobacteria_03_83	0,18	Bacteria;Proteobacteria;Gammaproteobacteria
78	Deferribacteres_03_4	0,18	Bacteria;Deferribacteres
79	Verrucomicrobia_03_28	0,17	Bacteria;Verrucomicrobia;Verrucomicrobiae;Verrucomicrobiales
80	Betaproteobacteria_03_9	0,18	Bacteria;Proteobacteria;Betaproteobacteria;Burkholderiales;Comamonadaceae
81	Deltaproteobacteria_03_122	0,17	Bacteria;Proteobacteria;Deltaproteobacteria
82	Alphaproteobacteria_03_32	0,17	Bacteria;Proteobacteria;Alphaproteobacteria
83	Alphaproteobacteria_03_329	0,17	Bacteria;Proteobacteria;Alphaproteobacteria
84	Gemmatimonadetes_03_1	0,17	Bacteria;Gemmatimonadetes
85	Gammaproteobacteria_03_46	0,17	Bacteria;Proteobacteria;Gammaproteobacteria
86	Actinobacteria_03_32	0,15	Bacteria;Actinobacteria;Actinobacteria
87	Alphaproteobacteria_03_264	0,16	Bacteria;Proteobacteria;Alphaproteobacteria
88	Verrucomicrobia_03_19	0,16	Bacteria;Verrucomicrobia;Opitutae;Opitutales;Opitutaceae;Opitutus
89	Gammaproteobacteria_03_198	0,14	Bacteria;Proteobacteria;Gammaproteobacteria
90	Alphaproteobacteria_03_195	0,15	Bacteria;Proteobacteria;Alphaproteobacteria
91	Deltaproteobacteria_03_74	0,15	Bacteria;Proteobacteria;Deltaproteobacteria
92	BacteriaNA_03_38	0,15	Bacteria
93	ProteobacteriaNA_03_51	0,14	Bacteria;Proteobacteria
94	Bacteroidetes_03_18	0,15	Bacteria;Bacteroidetes;Flavobacteria;Flavobacteriales
95	Planctomycetes_03_6	0,13	Bacteria;Planctomycetes;Planctomycetacia;Planctomycetales;Planctomycetaceae
96	Alphaproteobacteria_03_280	0,12	Bacteria;Proteobacteria;Alphaproteobacteria;Rickettsiales;SAR11
97	BacteriaNA_03_21	0,13	Bacteria
98	BacteriaNA_03_75	0,14	Bacteria
99	Actinobacteria_03_37	0,13	Bacteria;Actinobacteria;Actinobacteria
100	Gammaproteobacteria_03_32	0,12	Bacteria;Proteobacteria;Gammaproteobacteria

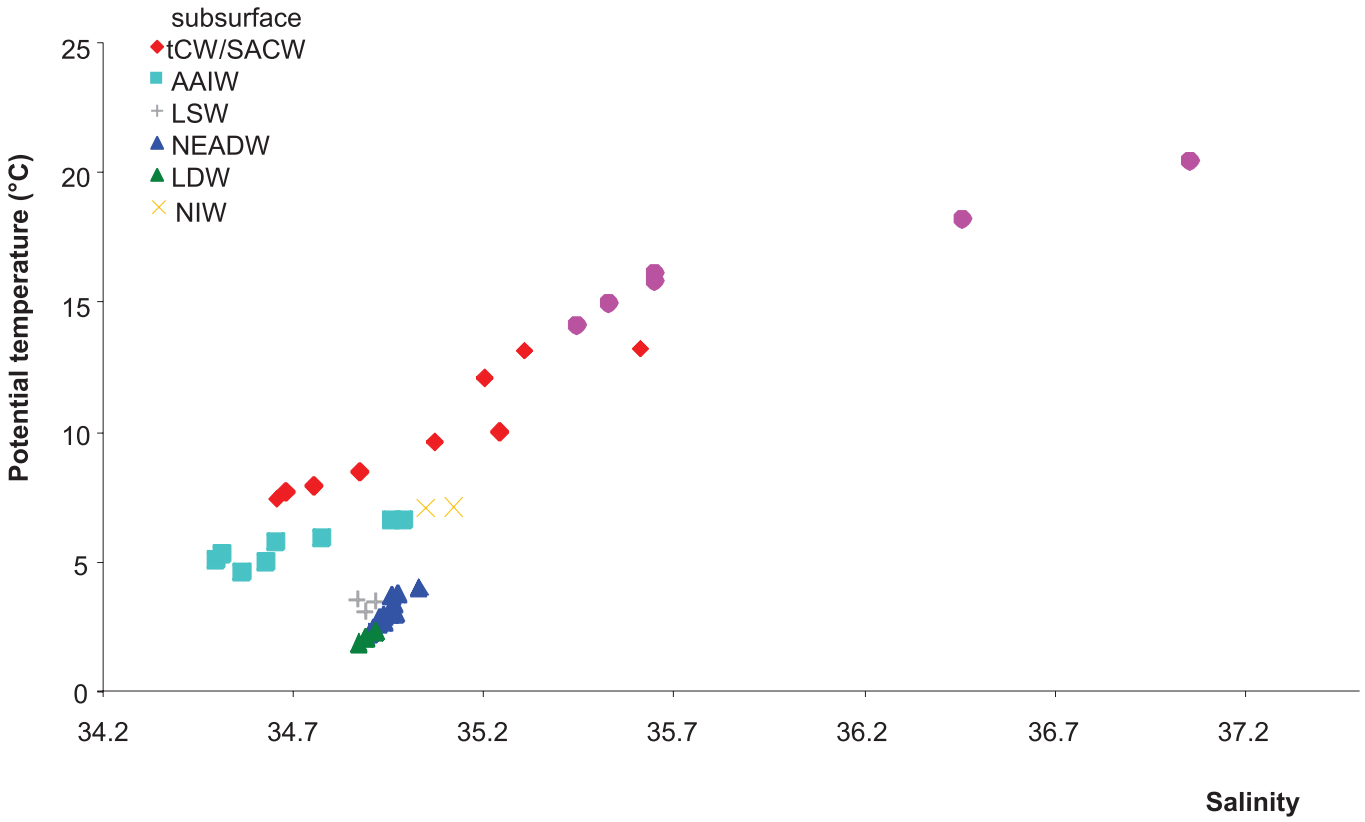

Figure S1. Temperature – salinity diagram based on all the samples. Different symbols indicate the different water masses (tCW/SACW: transitional/South Atlantic Central Water, AAIW: Antarctic Intermediate Water, LSW: Labrador Sea Water, NEADW: North East Atlantic Deep Water, LDW: Lower Deep Water).

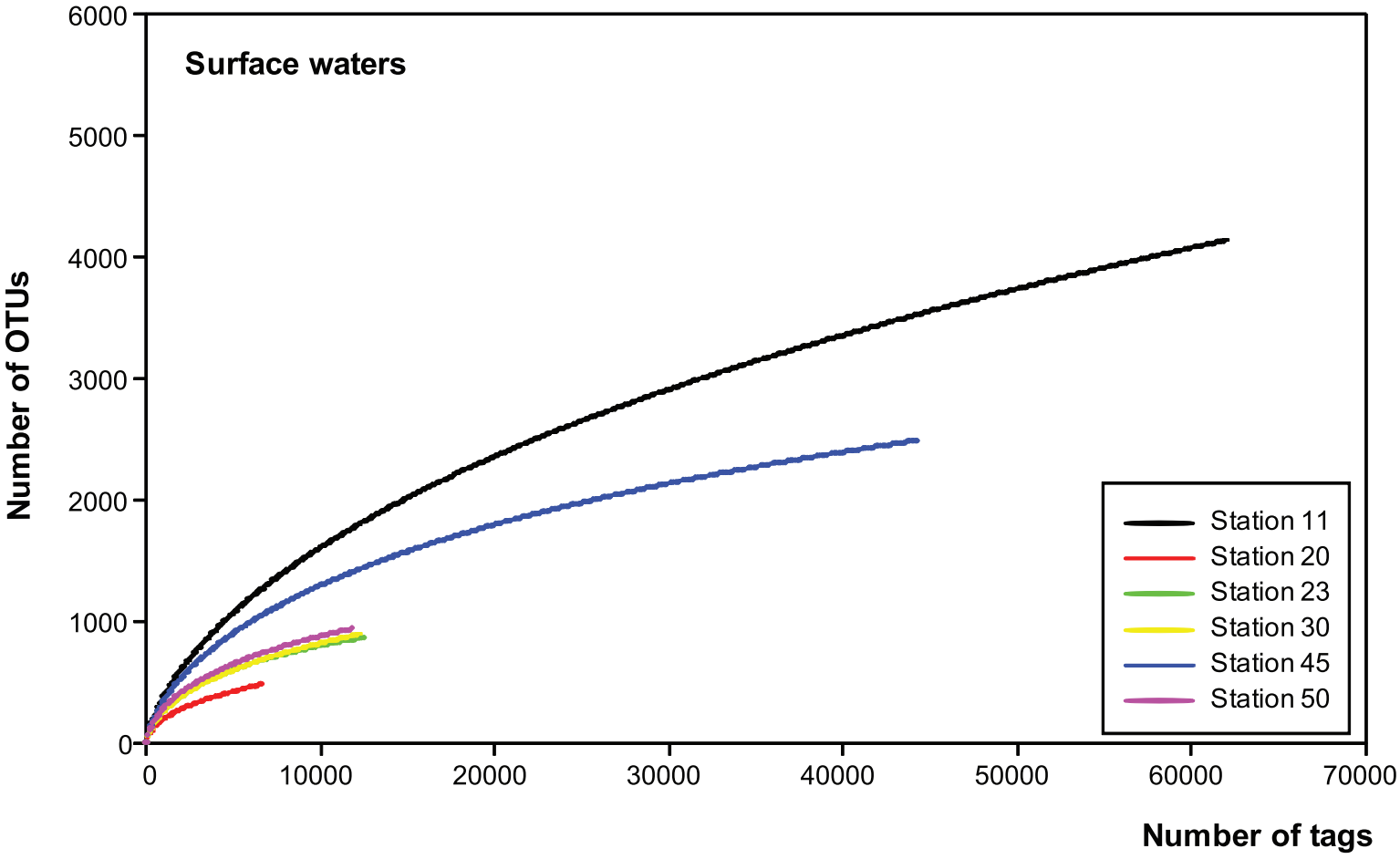

Figure S2 A. Rarefaction curves for subsurface (≈100 m depth) samples.

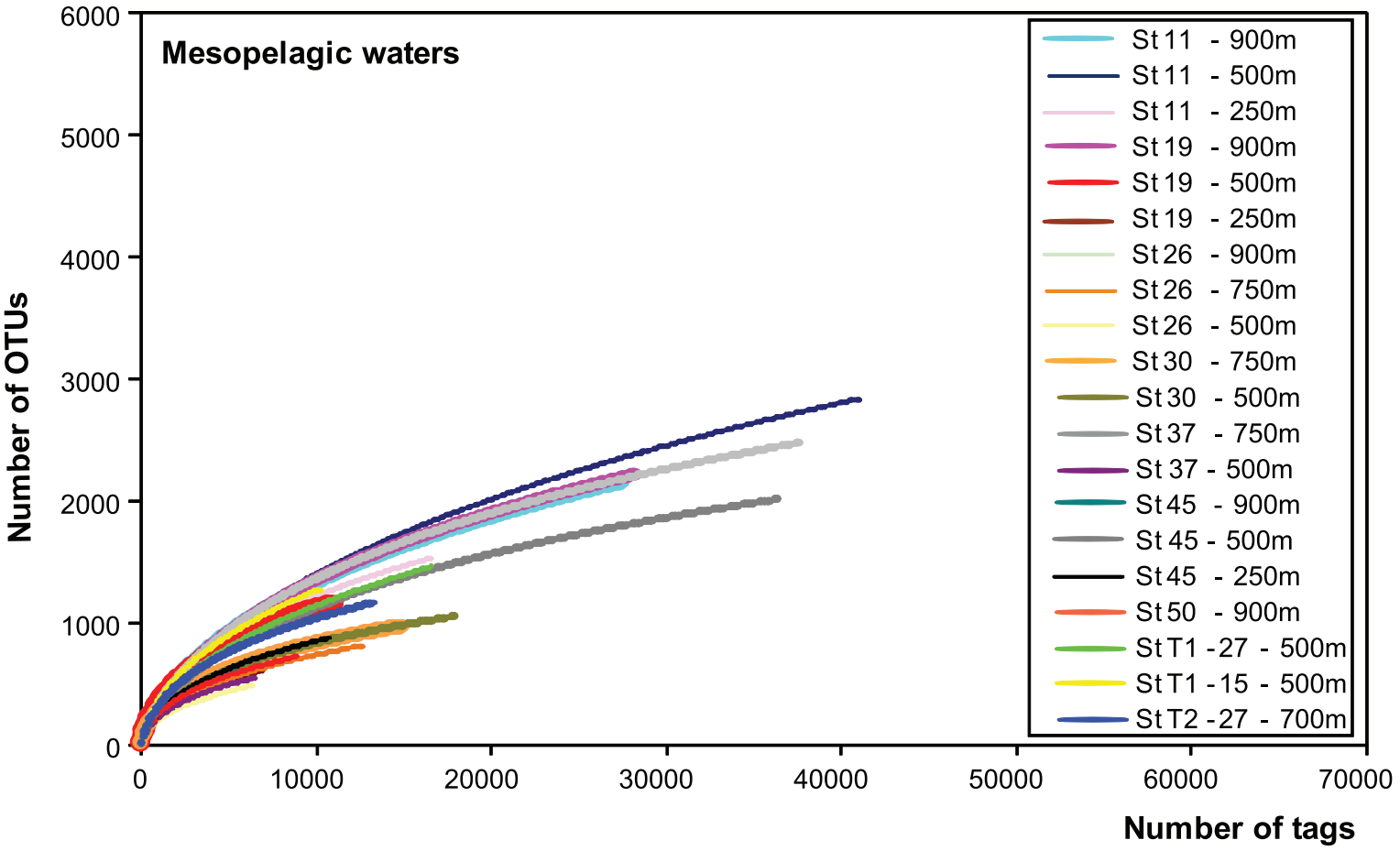

Figure S2 B. Rarefaction curves for mesopelagic samples.

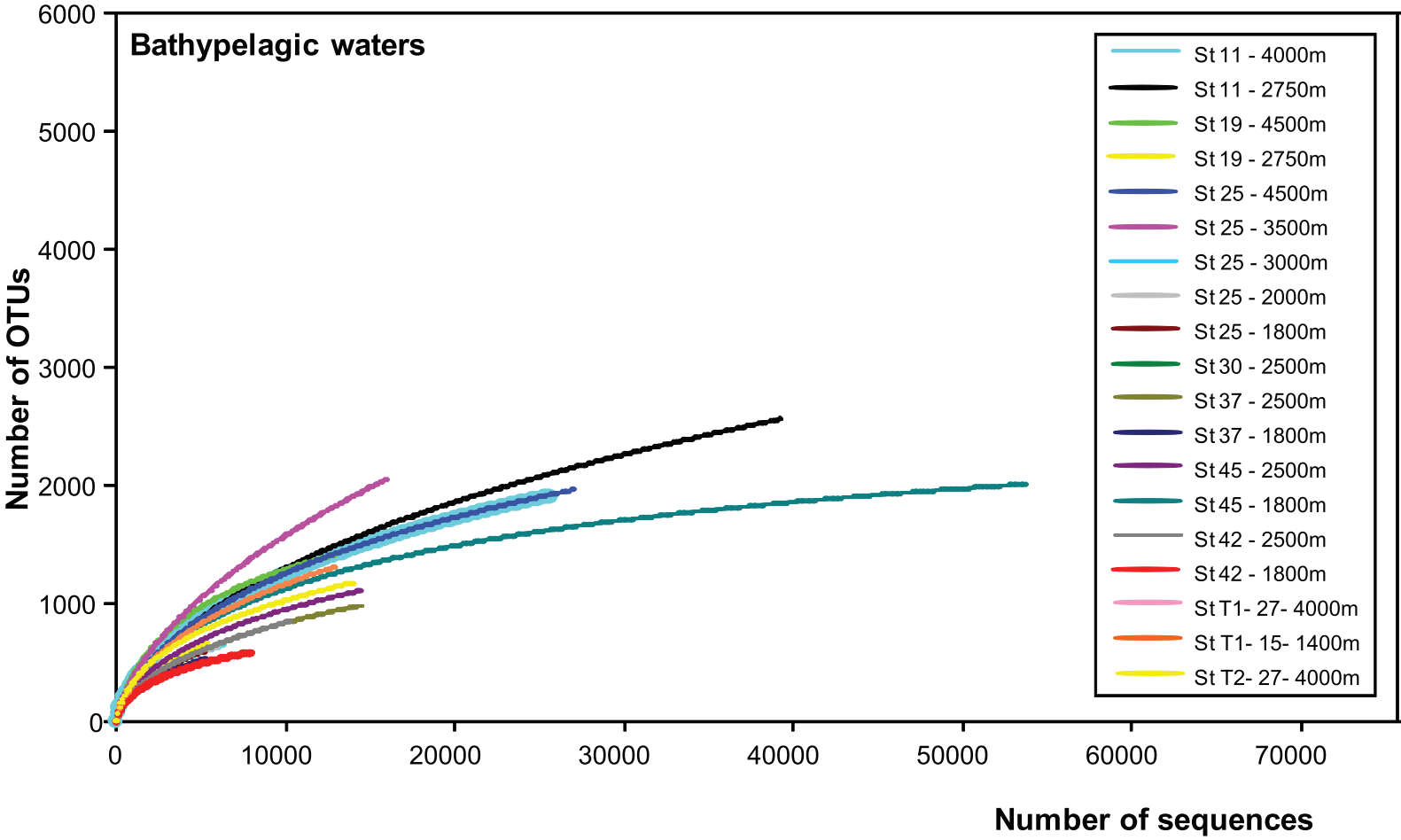

Figure S2 C. Rarefaction curves for bathypelagic samples.

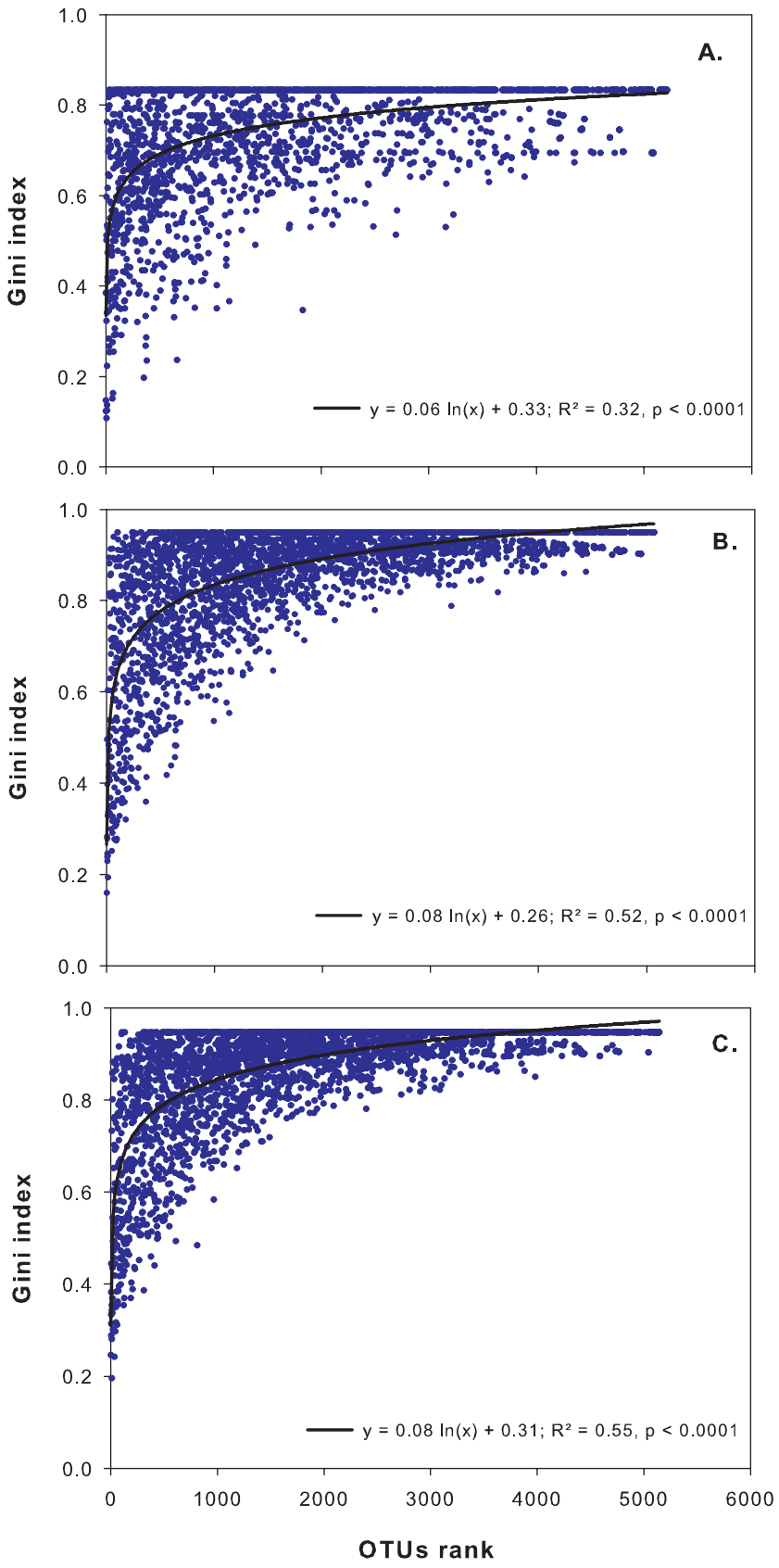

Figure S3. Evenness (Gini index) for each bacterial OTUs (97%) except the singletons from (A) subsurface, (B) mesopelagic and (C) bathypelagic samples vs. the rank (based on the relative abundance) of that OTU. A Gini index of 1 would indicate a very uneven OTU whereas a Gini index of 0 would indicate a perfectly even OTU.

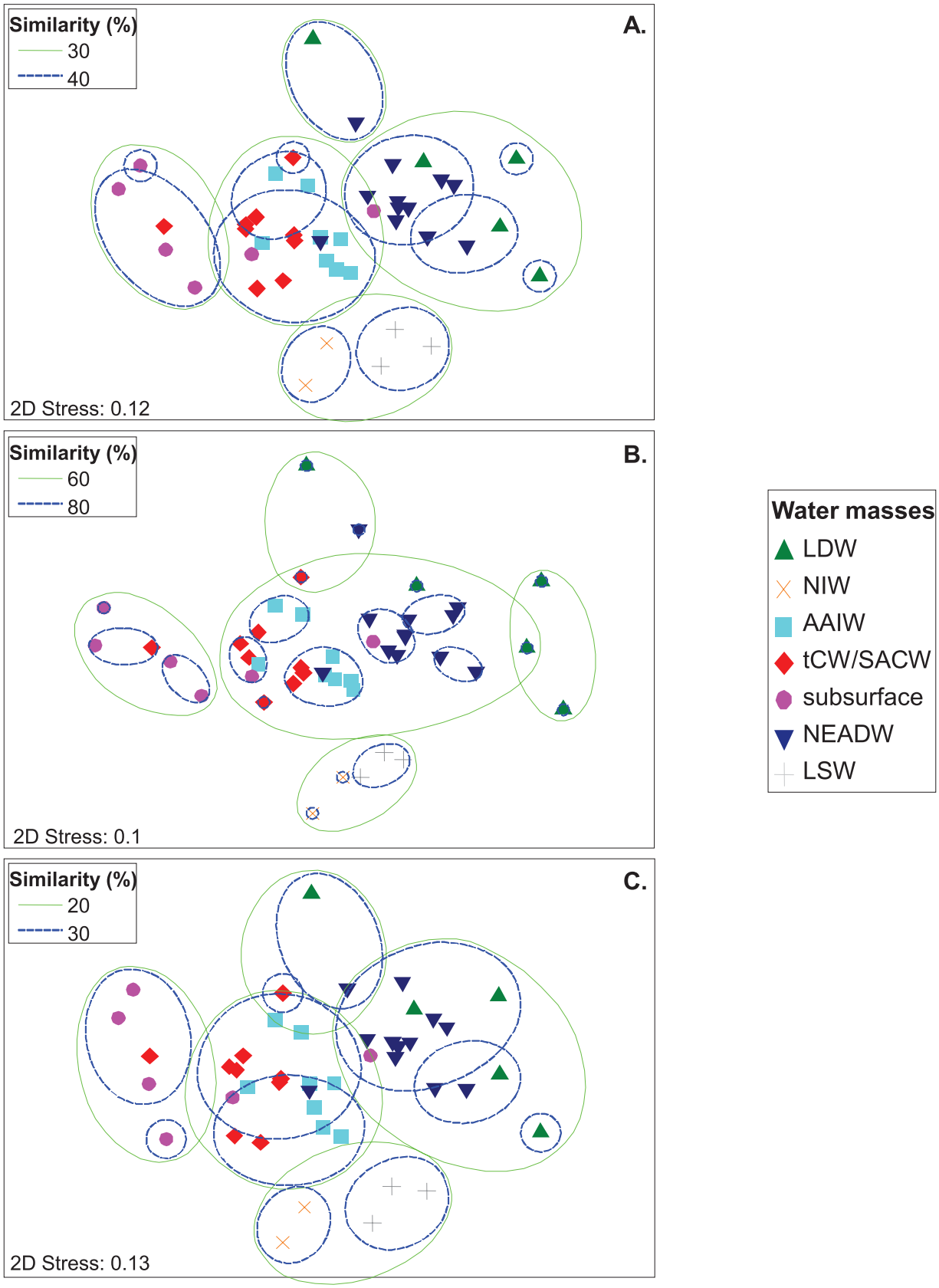

Figure S4. Non-metric multidimensional analysis based on relative abundance of (A) all pyrotags except the singletons, (B) abundant pyrotags (frequency > 1% within a sample) and (C) rare pyrotags (frequency < 0.1% within a sample). Individual samples were affiliated to their respective water-mass. Superimposed circles represent clusters of samples at similarity values of (A) 30 and 40%, (B) 60 and 80% and (C) 20 and 30% (Bray-Curtis similarity). The final solution was based on 25 iterations with a final stress of (a) 0.10 and (b) 0.13.

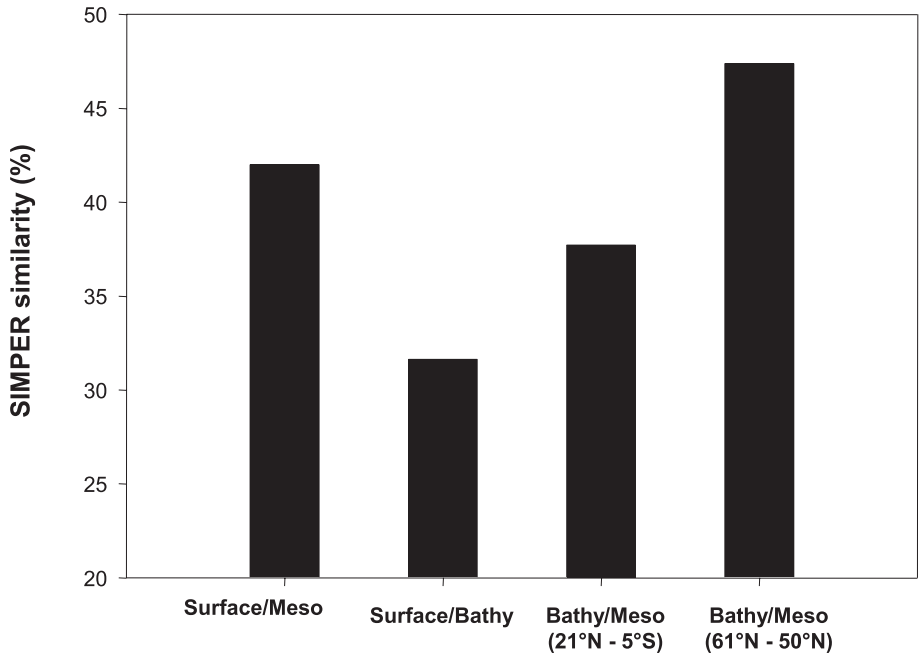

Figure S5. Percent of similarity (calculated through SIMPER analysis) between depth zones.